Investigation of Helicopter Rotor Blade Tip Vortices in Wind Tunnels and in Flight

Markus Raffel et al.

DLR Institute of Aerodynamics and Flow Technology, Göttingen

DLR
Deutsches Zentrum
für Luft- und Raumfahrt e.V.
in der Helmholtz-Gemeinschaft

Typical features of helicopter rotor blade aerodynamics

Particle Image Velocimetry

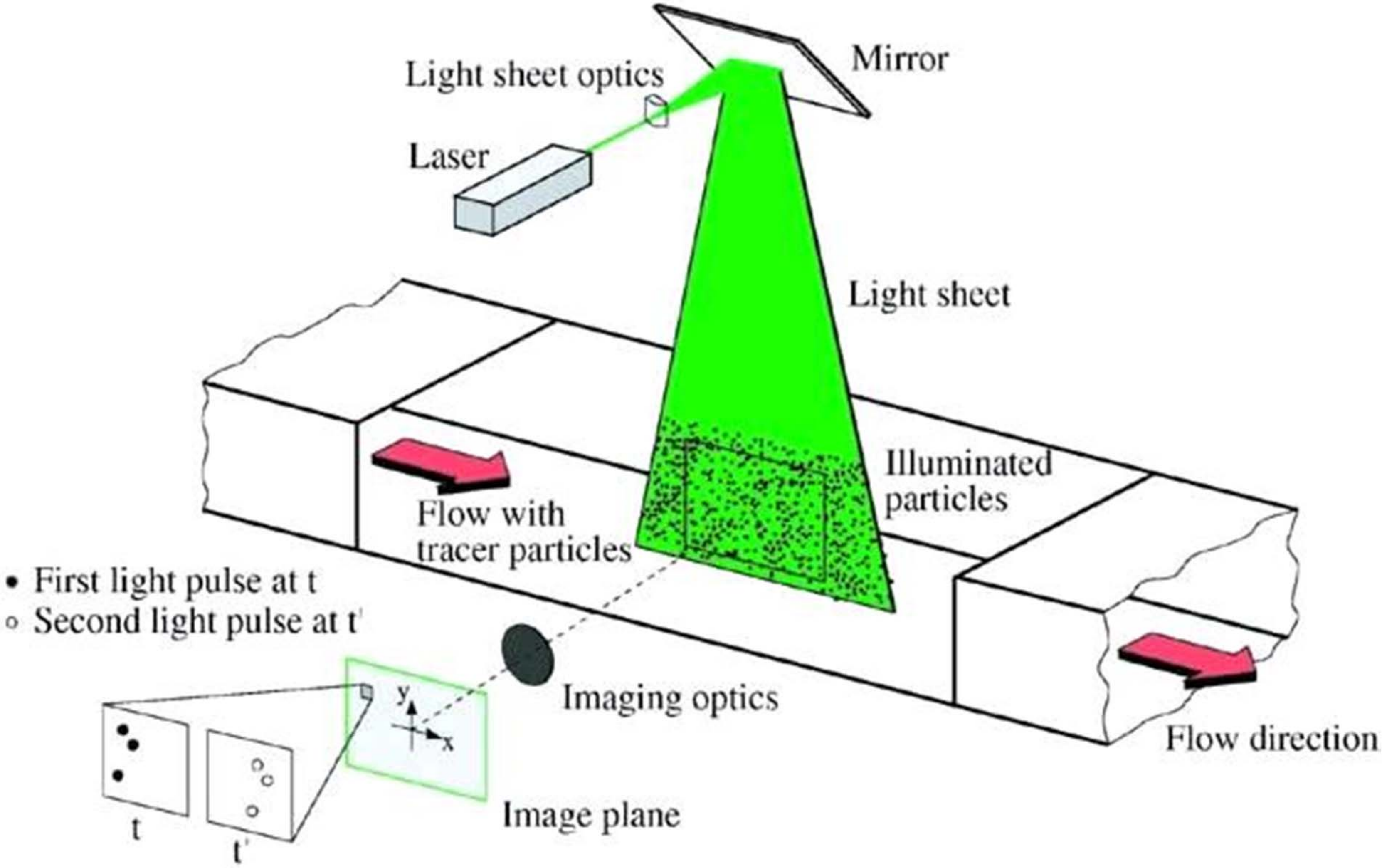

From: Raffel, Willert, Kompenhans: Particle Image Velocimetry, Springer-Verlag 1997

The complex interaction of blade tip vortex and dynamical stall flow regions is very hard to predict numerically

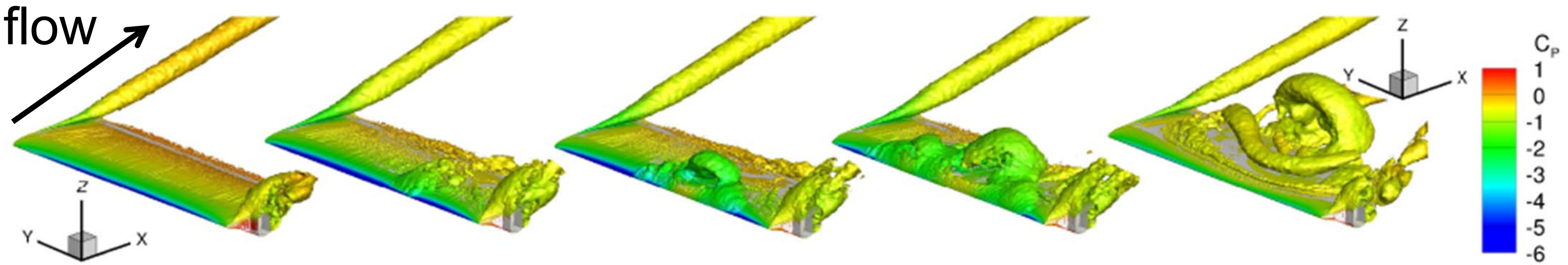

Fig. 17: Dynamic stall evolution around the OA209 wing: the DLR-TAU computations with Menter SST turbulence model. Visualized by means of isosurfaces of the λ_2 criterion. From left to right: α=17.2°↑, α=21.2°↓, α=20.6°↓, α=19.8°↓, α=16.8°↓.

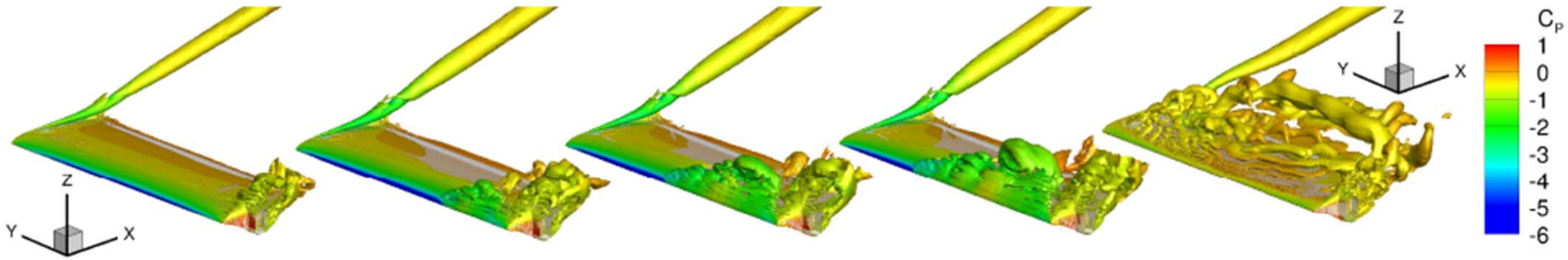

Fig. 18: Dynamic stall evolution around the OA209 wing: the elsA computations with k-ω Kok + SST turbulence model. Visualized by means of isosurfaces of the λ_2 criterion. From left to right: α=17.5°↑, α=21.3°↑, α=21.8°↑, α=21.9°↑, α=17.5°↓.

Pitching blade tip wind tunnel experiments

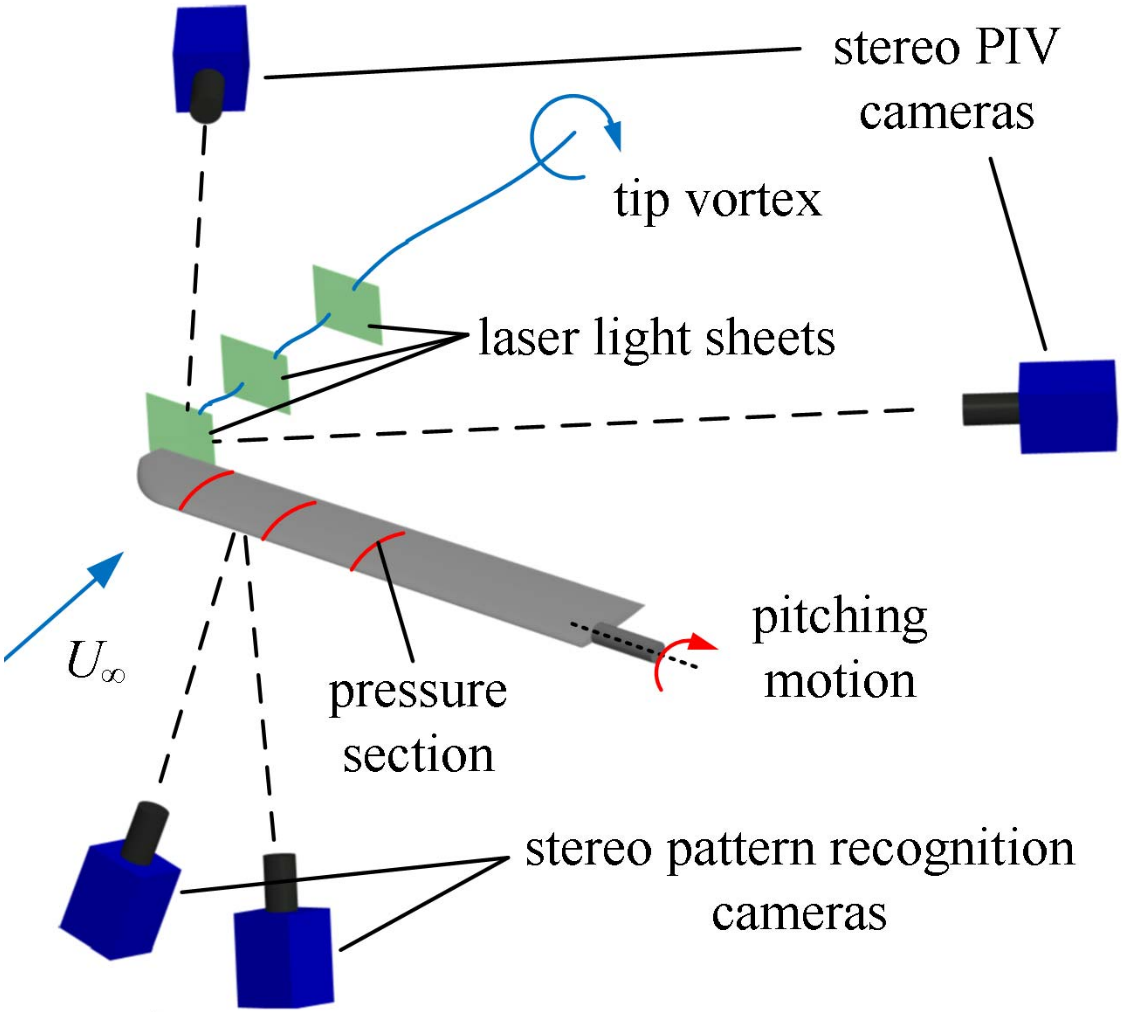

- 2 kHZ framing rate stereo PIV
- simultaneous stereoscopic blade deflection measurements
- simultaneous unsteady pressure measurements with 196 kulites
- 6 components piezzo balance
- free-stream Mach number 0.15
- pitching frequencies 5Hz-10Hz

Time-averaged results for static AoA

- Streamwise velocity u and planar (v,w)-streamlines

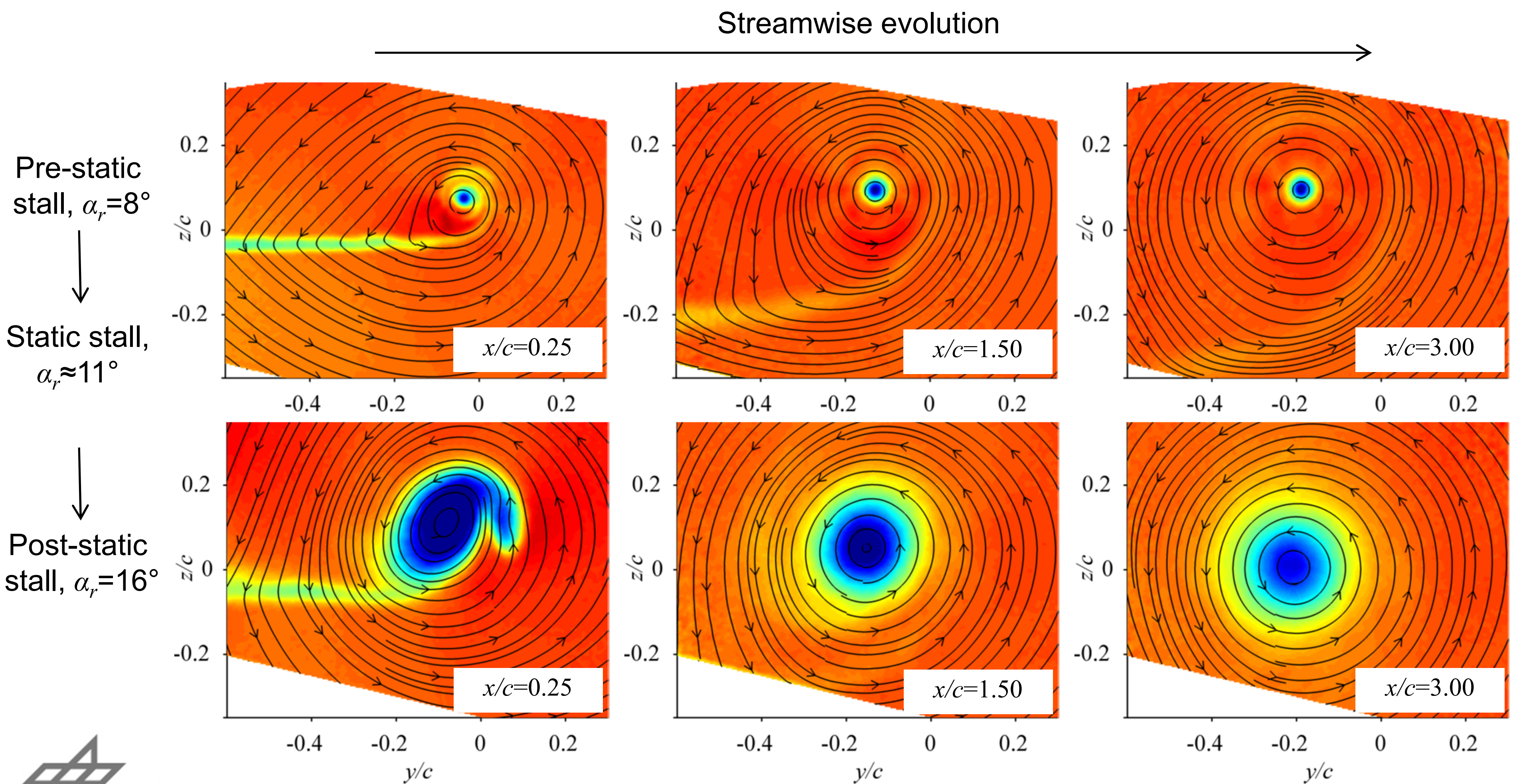

Time-averaged swirl velocity and circulation for static AoA

- The **swirl velocity** u_θ and the corresponding **circulation** $\Gamma = 2\pi r u_\theta$ were determined
  for each instantaneous flow field (accounting for unsteady vortex motion)
- Time-averaged results for pre- and post-stall ($\alpha_r = 8°, 16°$):

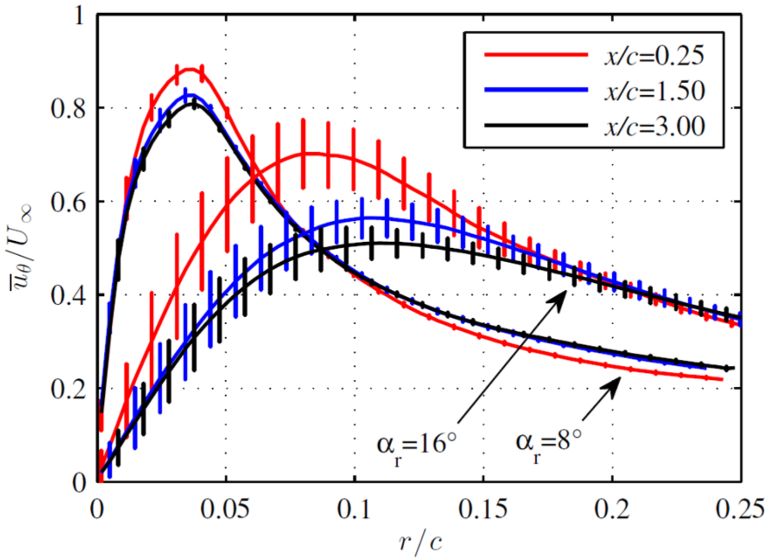

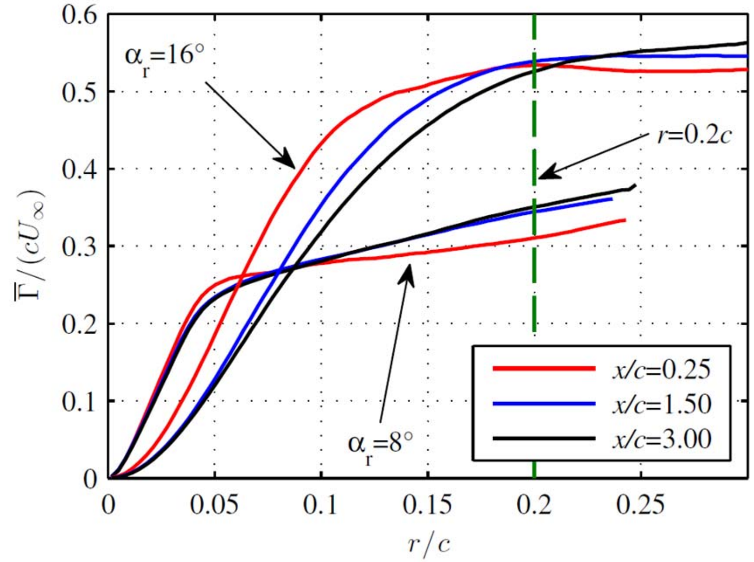

Swirl velocity u_θ (+standard deviation) Circulation Γ

Example flow fields for a deep-stall test case

- Pitch oscillations: α_r=11°±6°, k=0.075

upstroke

downstroke

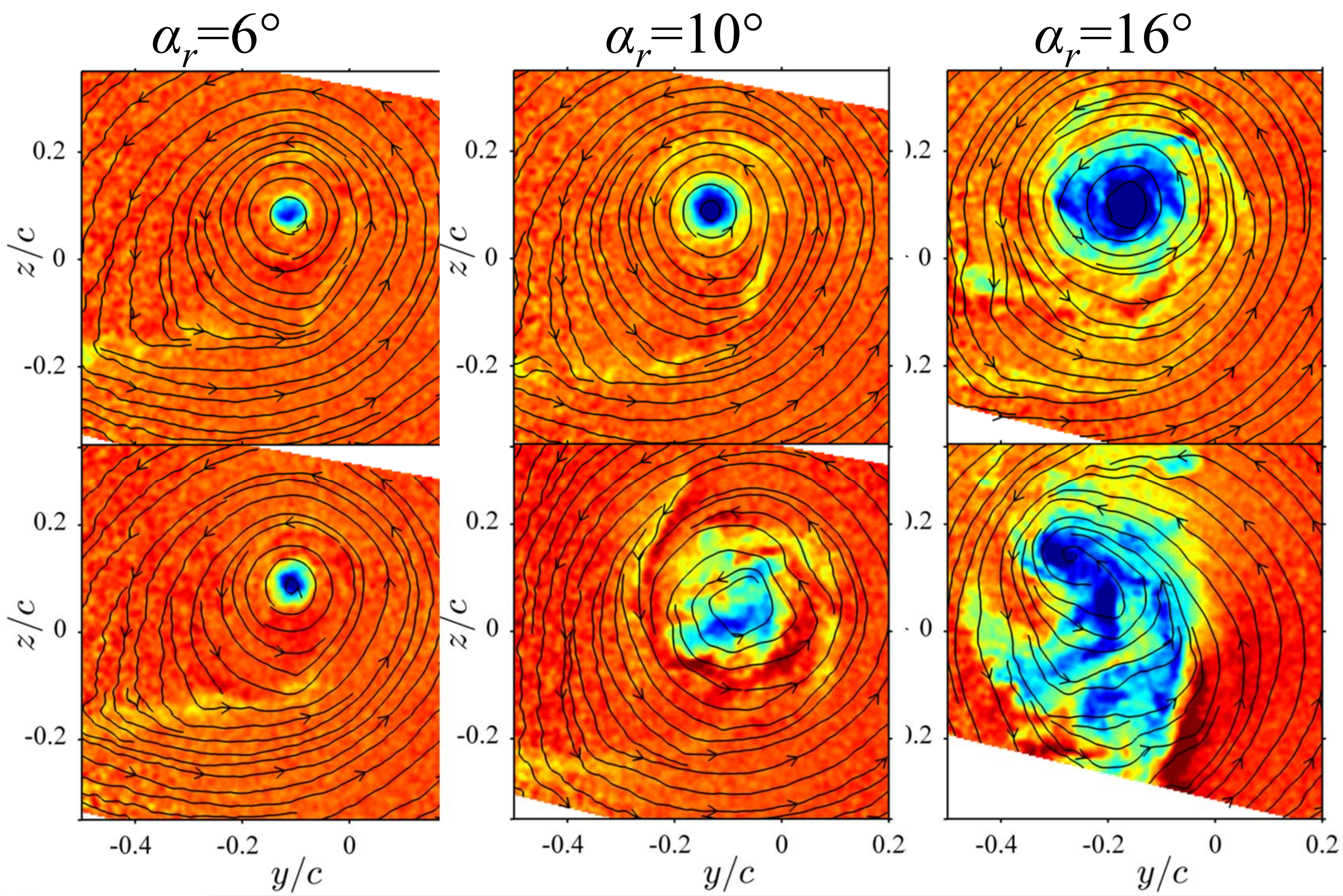

Phase-averaged dynamic results

- **Phase-lag correction**, accounting for the vortex convection from the tip's TE to the measurement plane

α_r=11°±6°, k=0.050

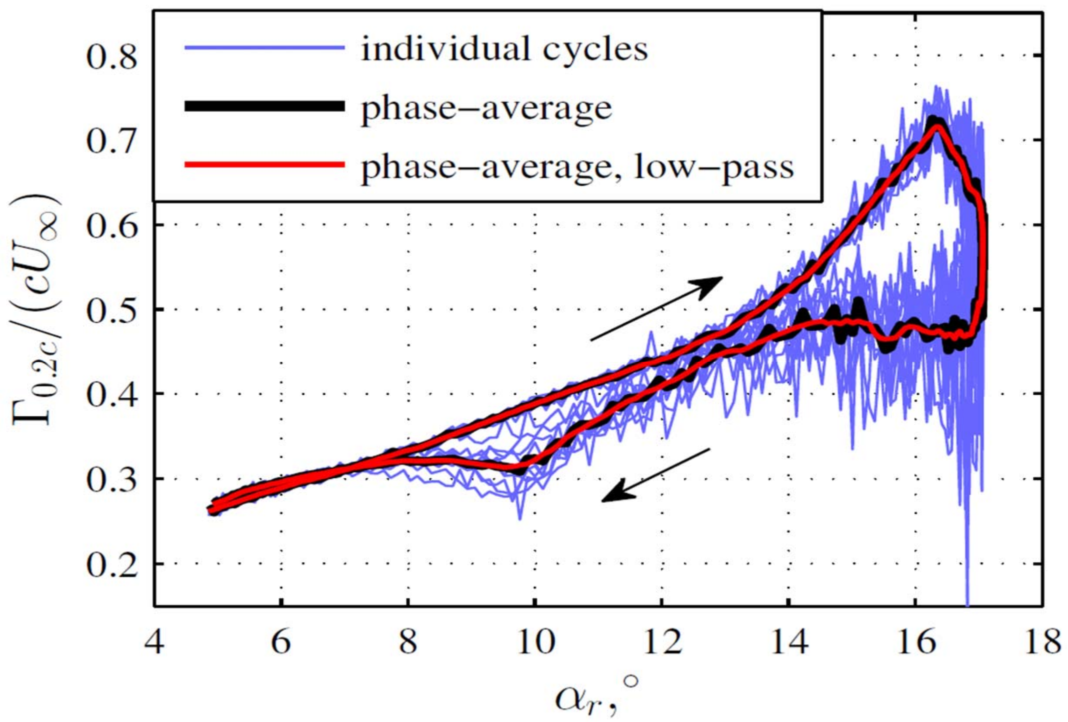

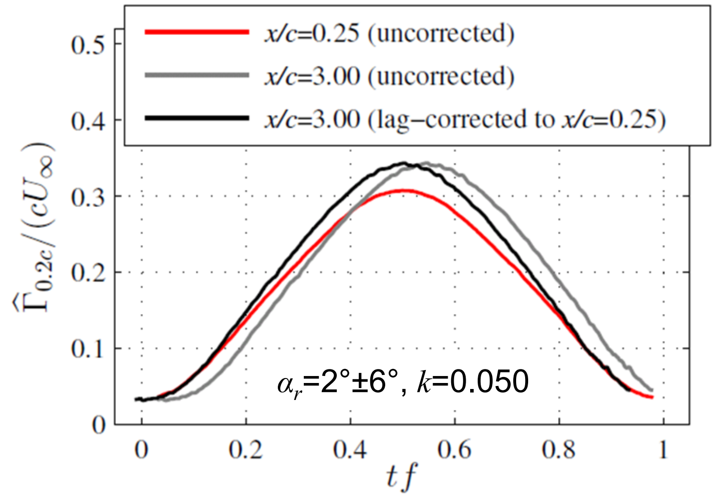

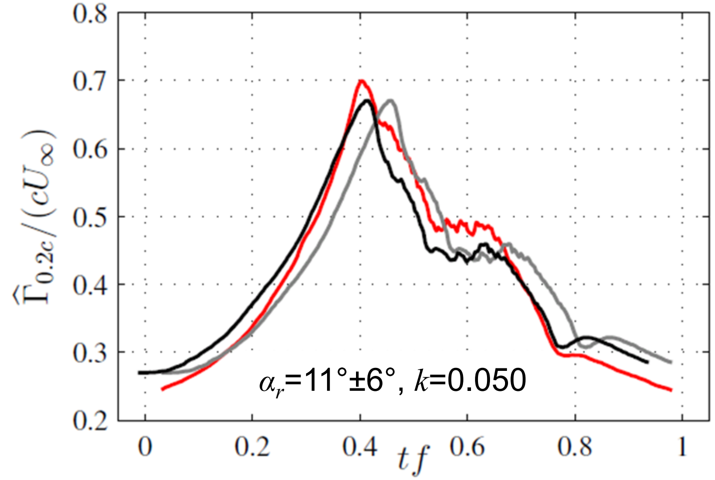

- **Phase-averaged circulation** for 10 pitch cycles

PIV measurements in the EU-project GOAHEAD

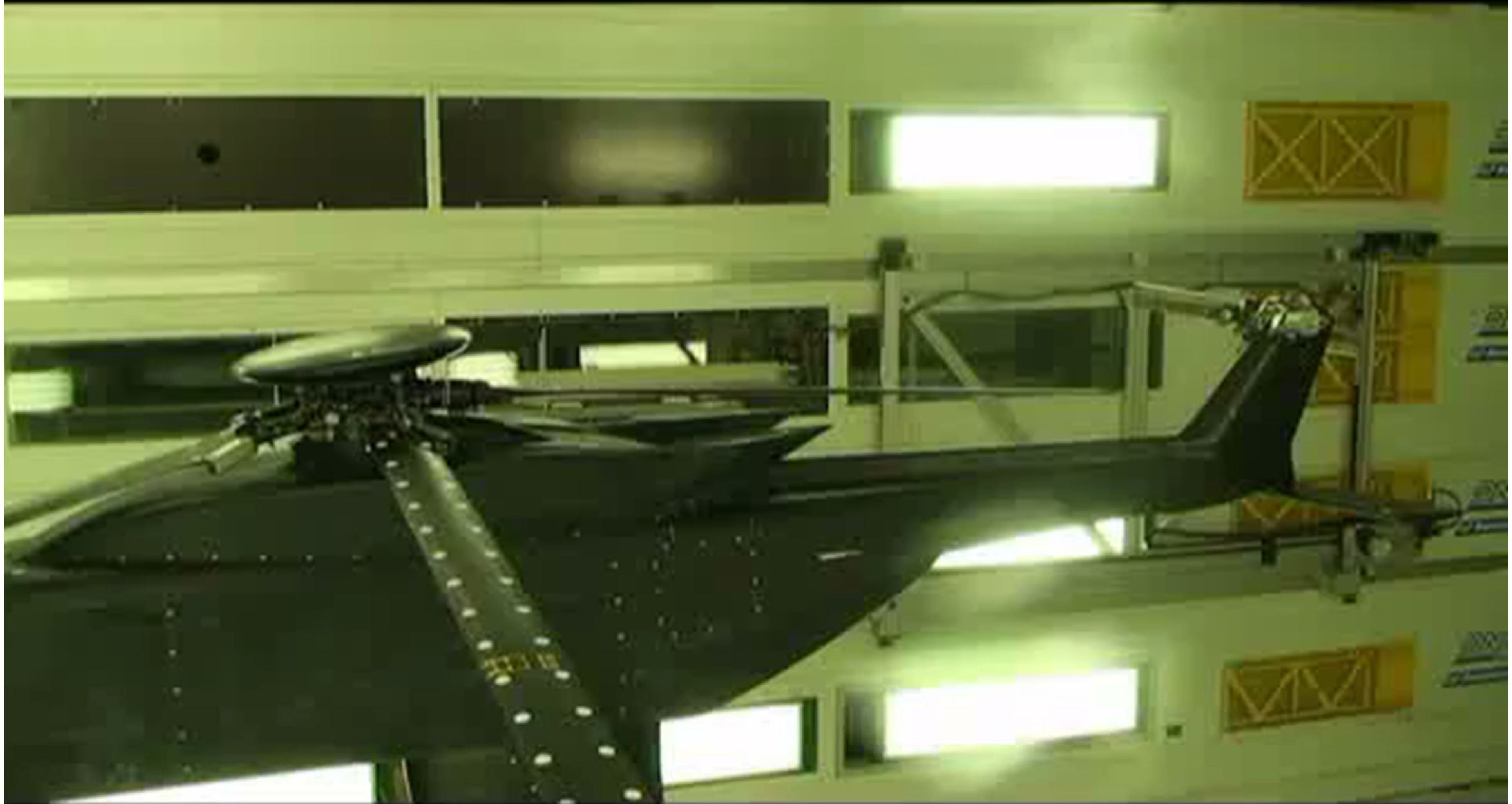

Volume scanning with PIV
(with and without rotor blades)

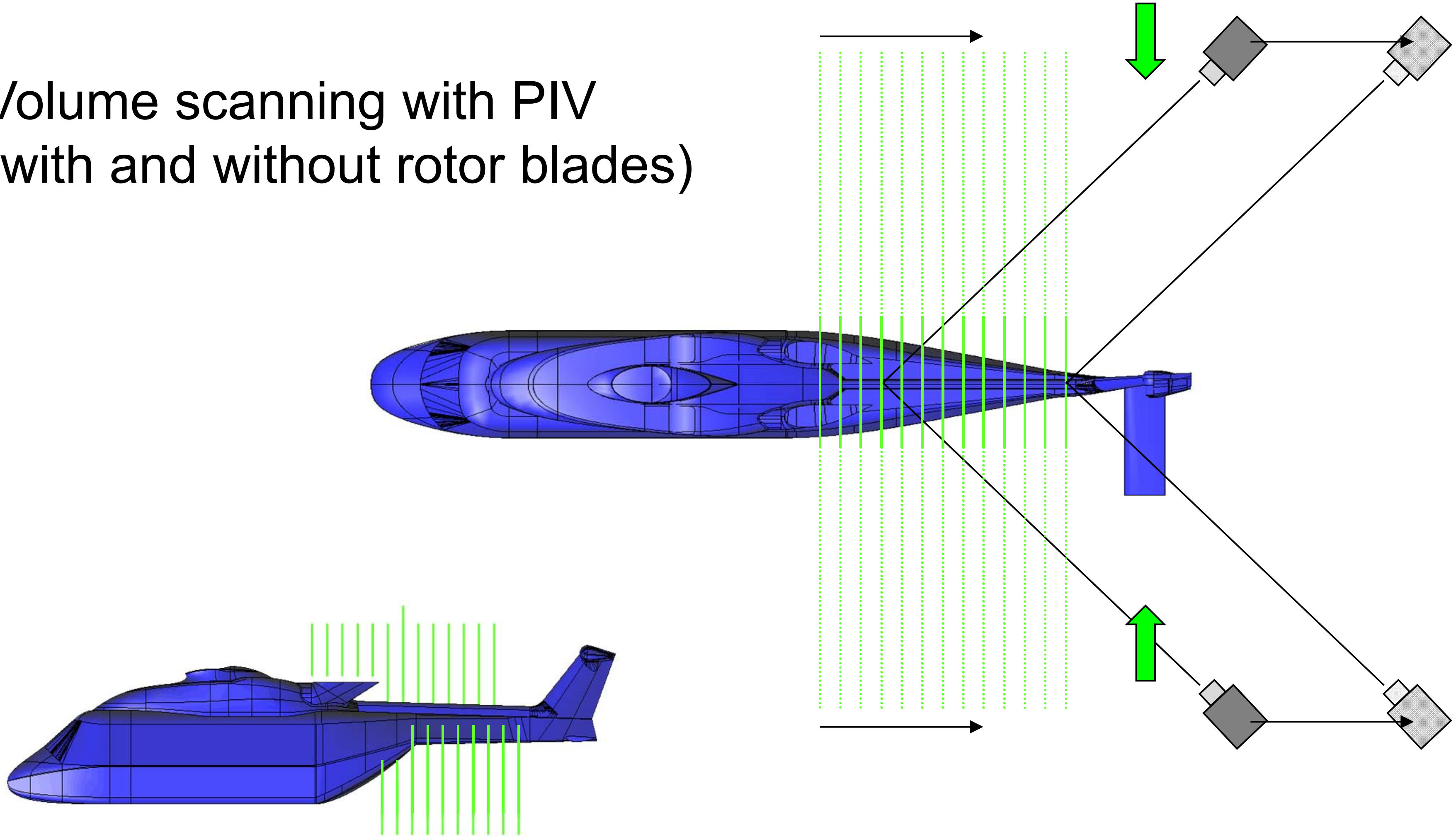

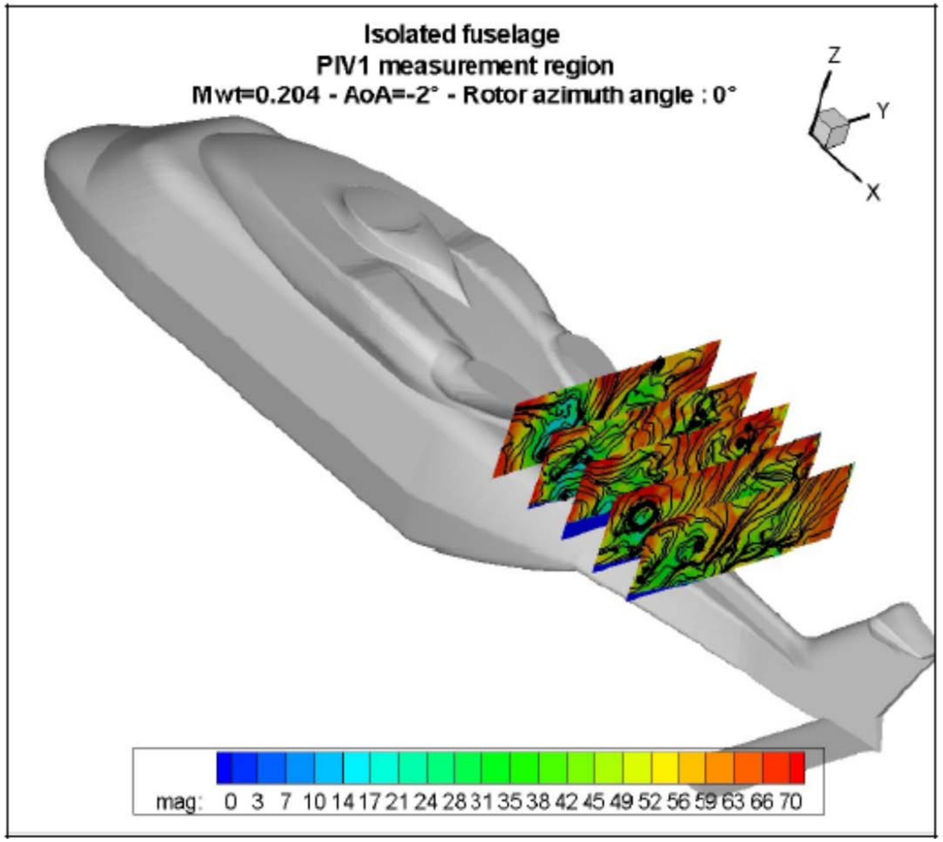

Figure11: TC1 – PIV1 - Isolated fuselage ΨMR=0°

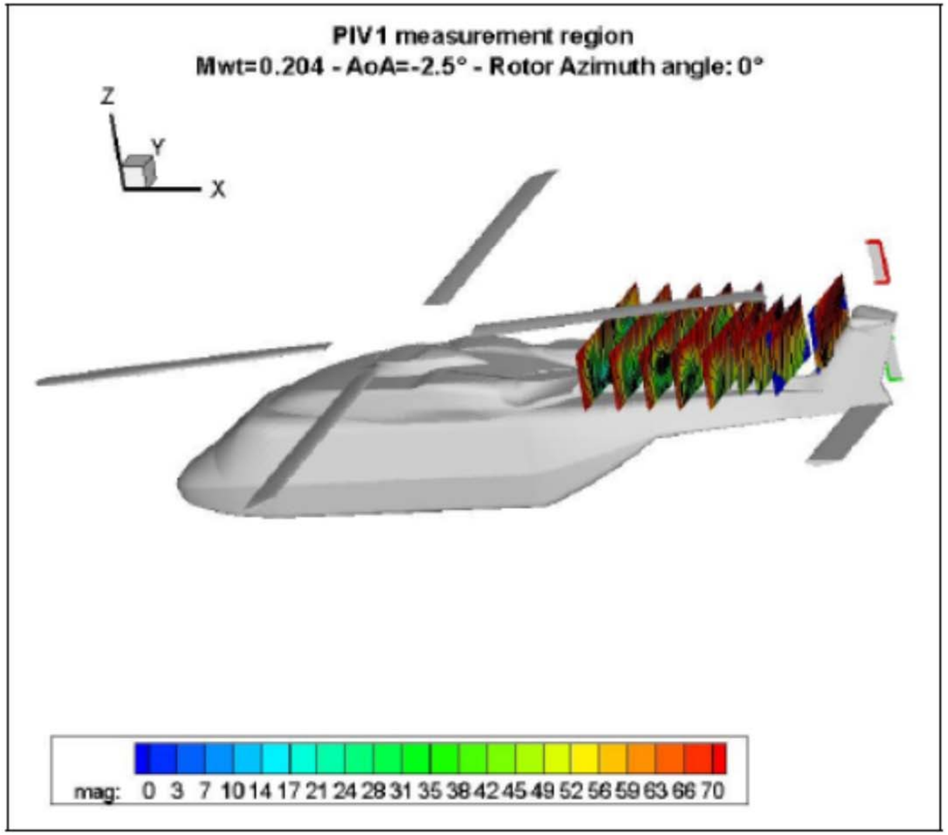

Figure12: TC3-4 –PIV1 -Full model for ΨMR=0°

The complex structure of the overall rotor wake, especially the vortex positons and strengths, is very hard to predict numerically

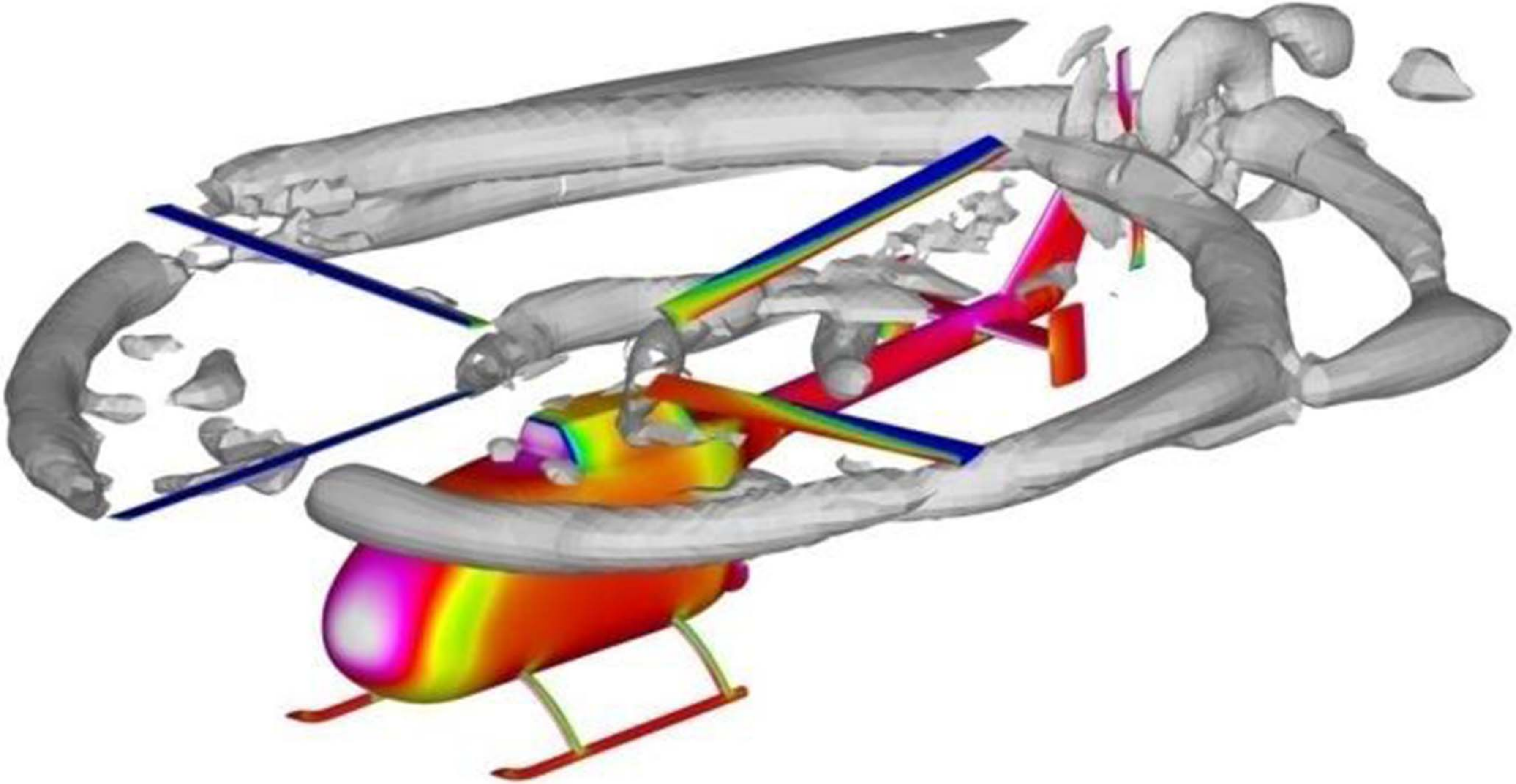

Visualization of rotor blade tip vortices (Werlé)

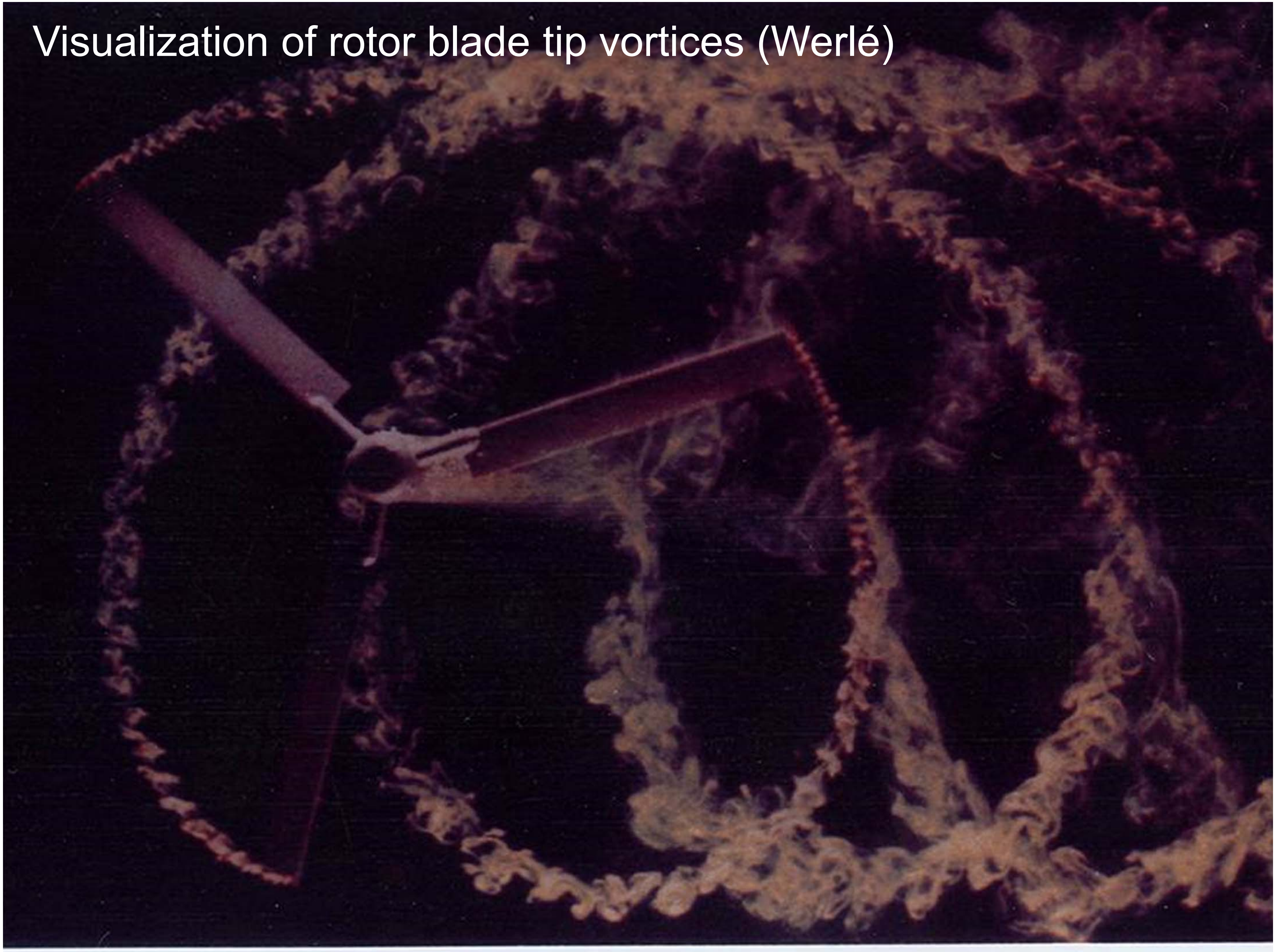

3D-simulation of helicopter blade tip vortices by a free wake code

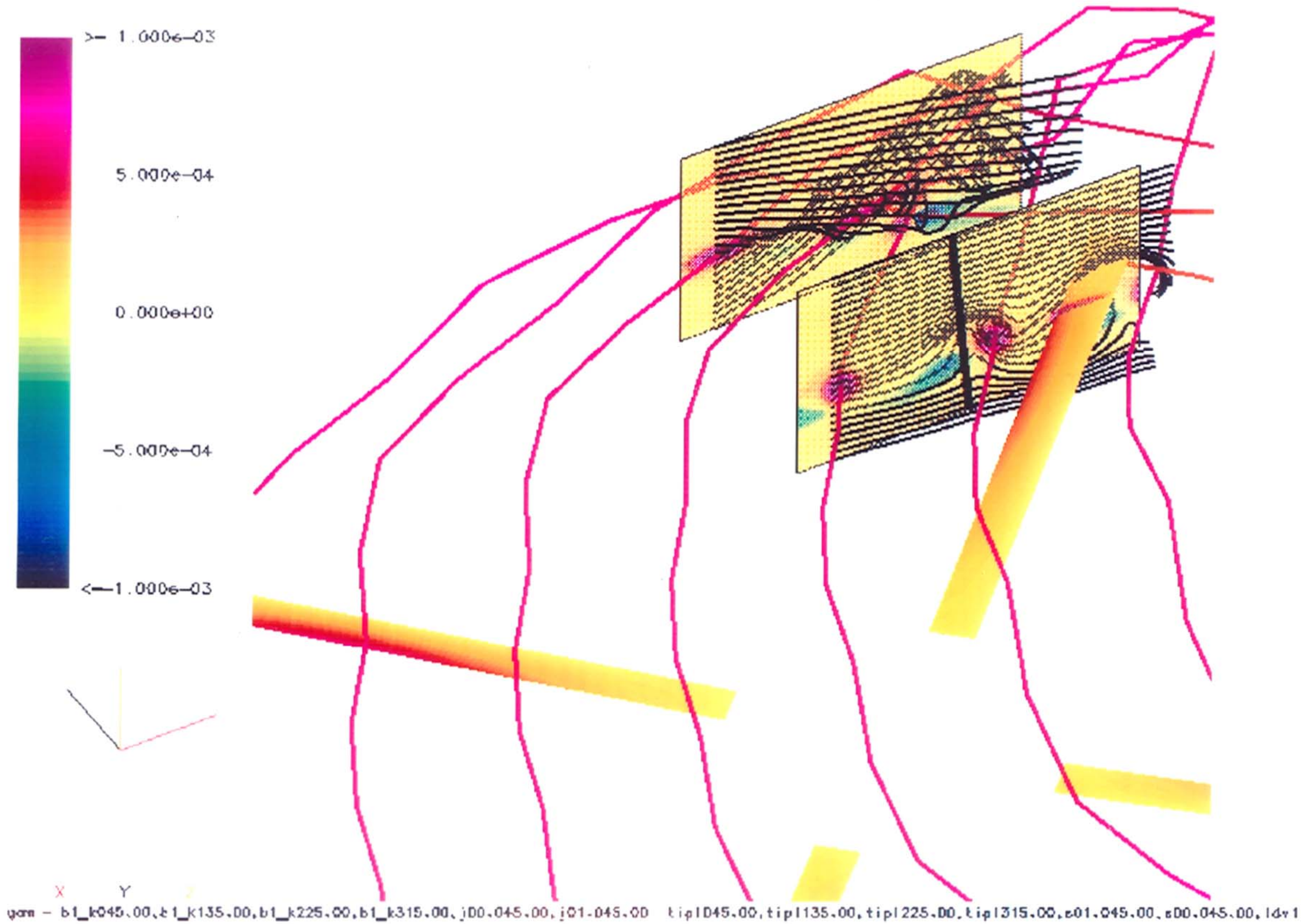

Unsteady pressure at the rotor blade and corresponding noise level at the ground (HARTII)

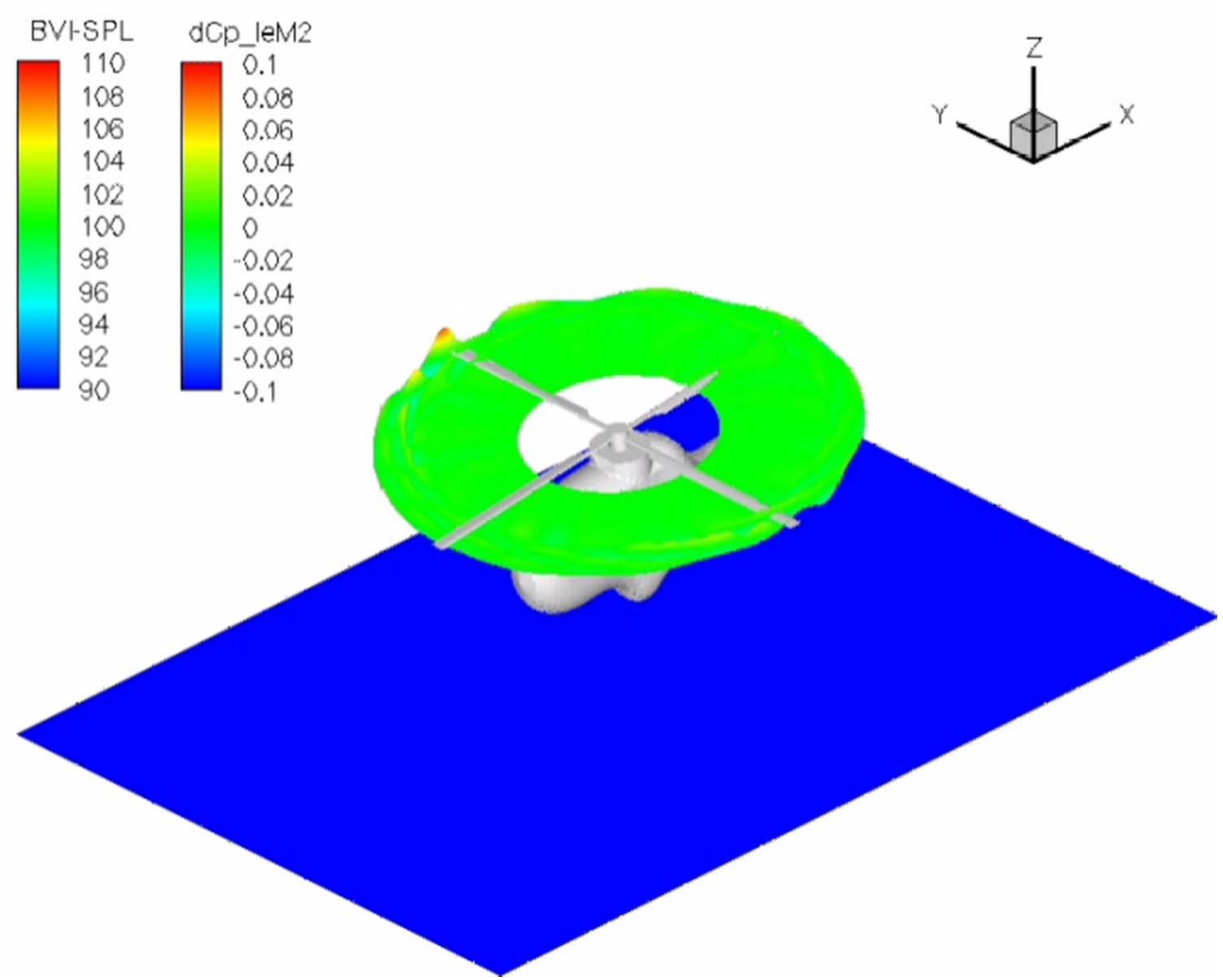

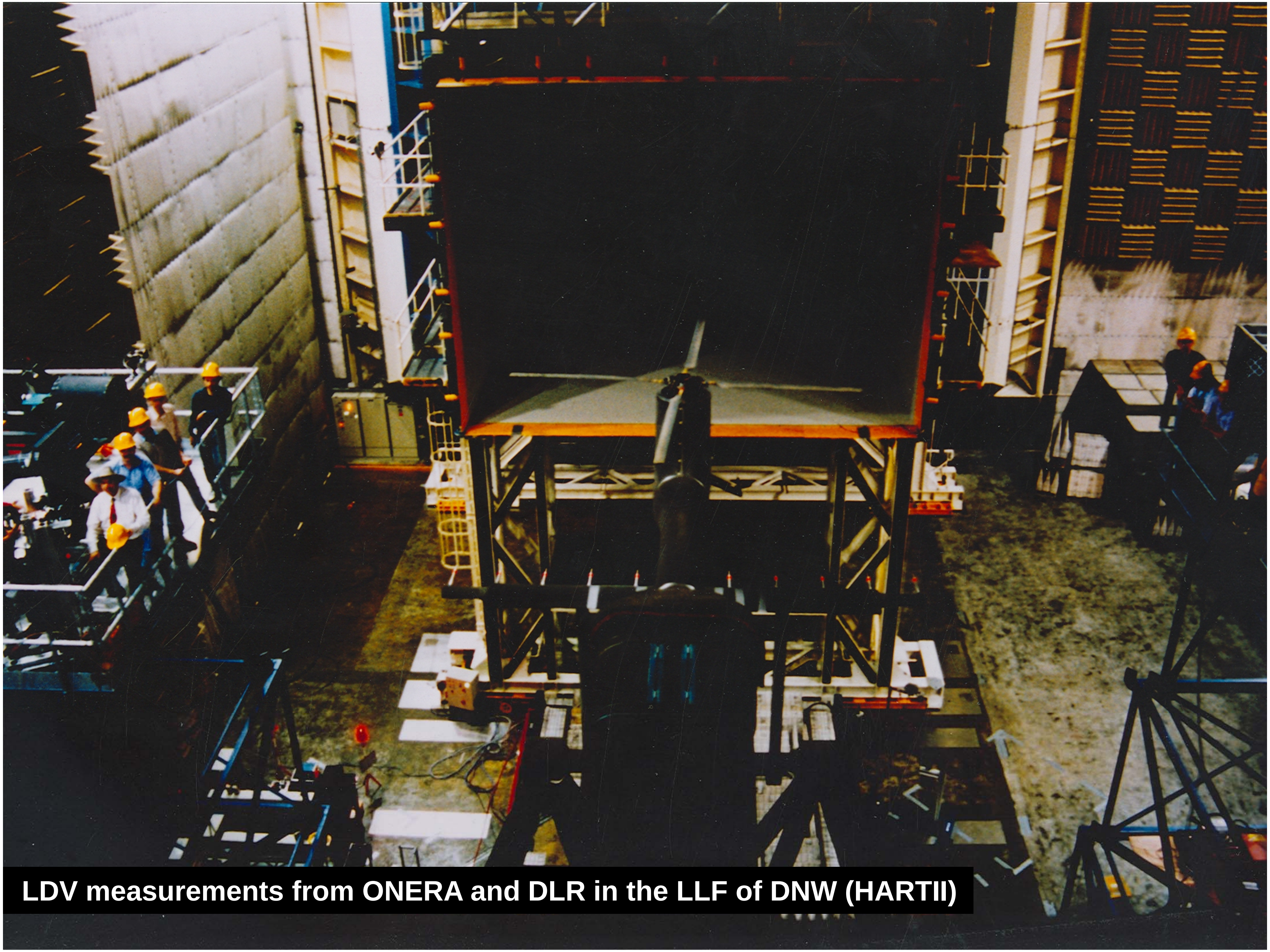

LDV measurements from ONERA and DLR in the LLF of DNW (HARTII)

PIV cameras systems and common support (HartII)

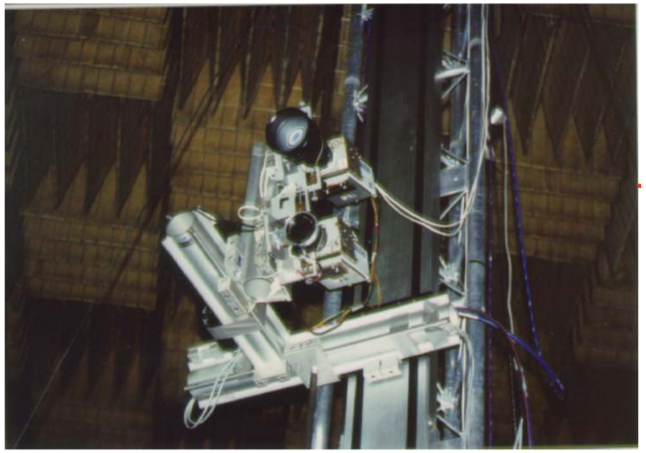

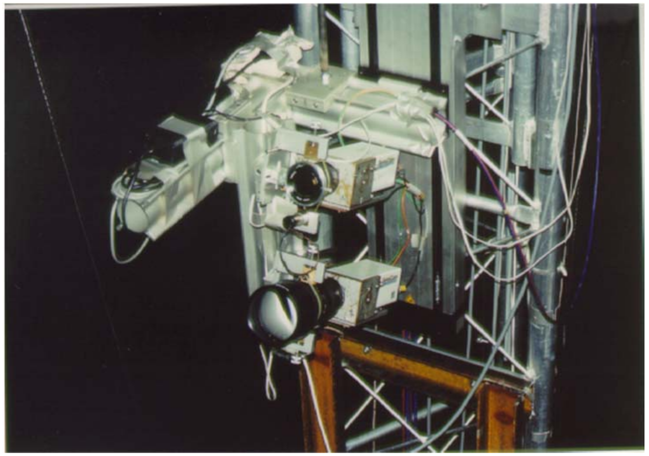

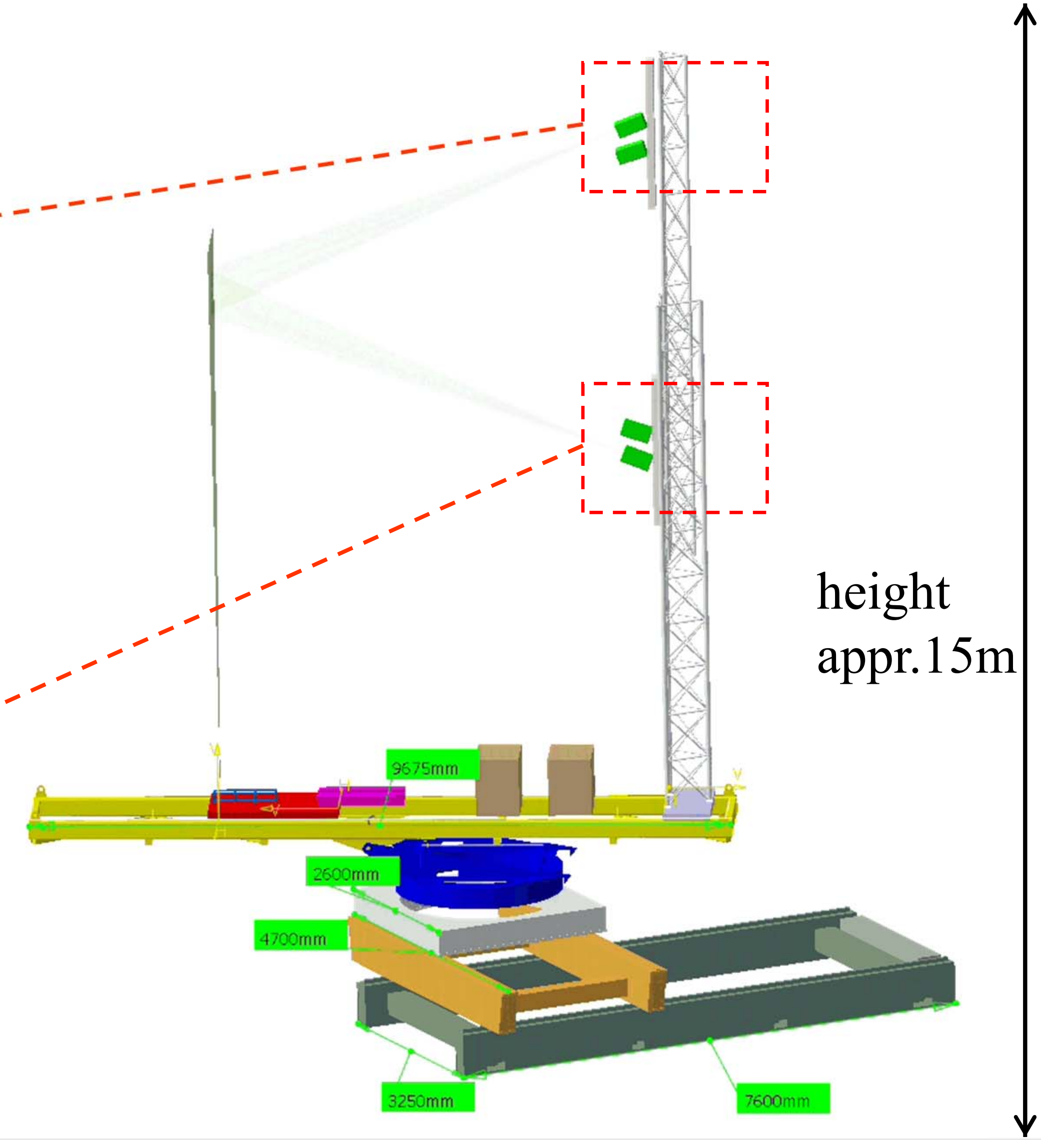

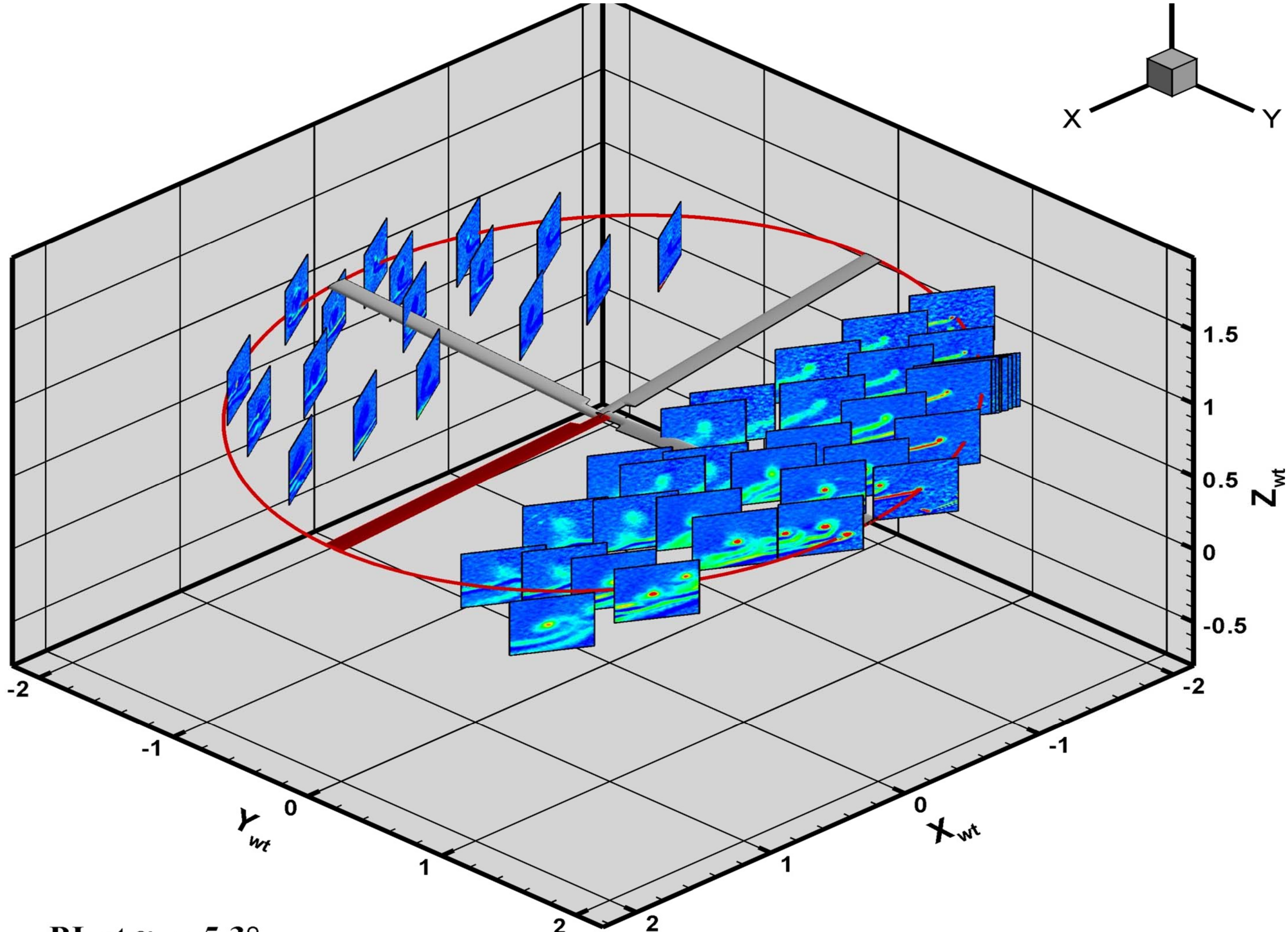

BL at $\alpha_s = 5.3°$

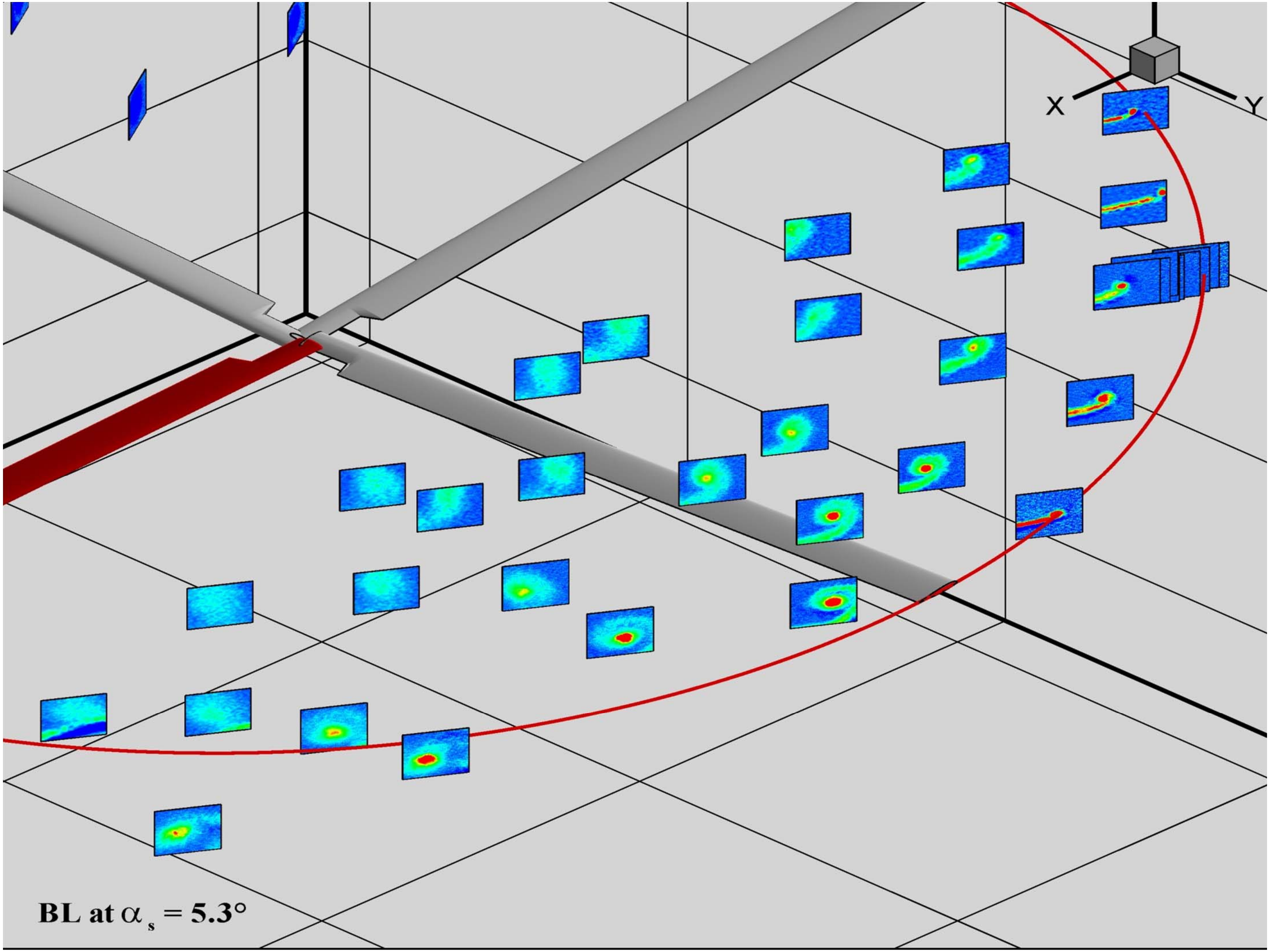
X
Y
BL at $\alpha_s = 5.3°$

stereoscopic PIV measurements of the tip vortices at hover flight conditions

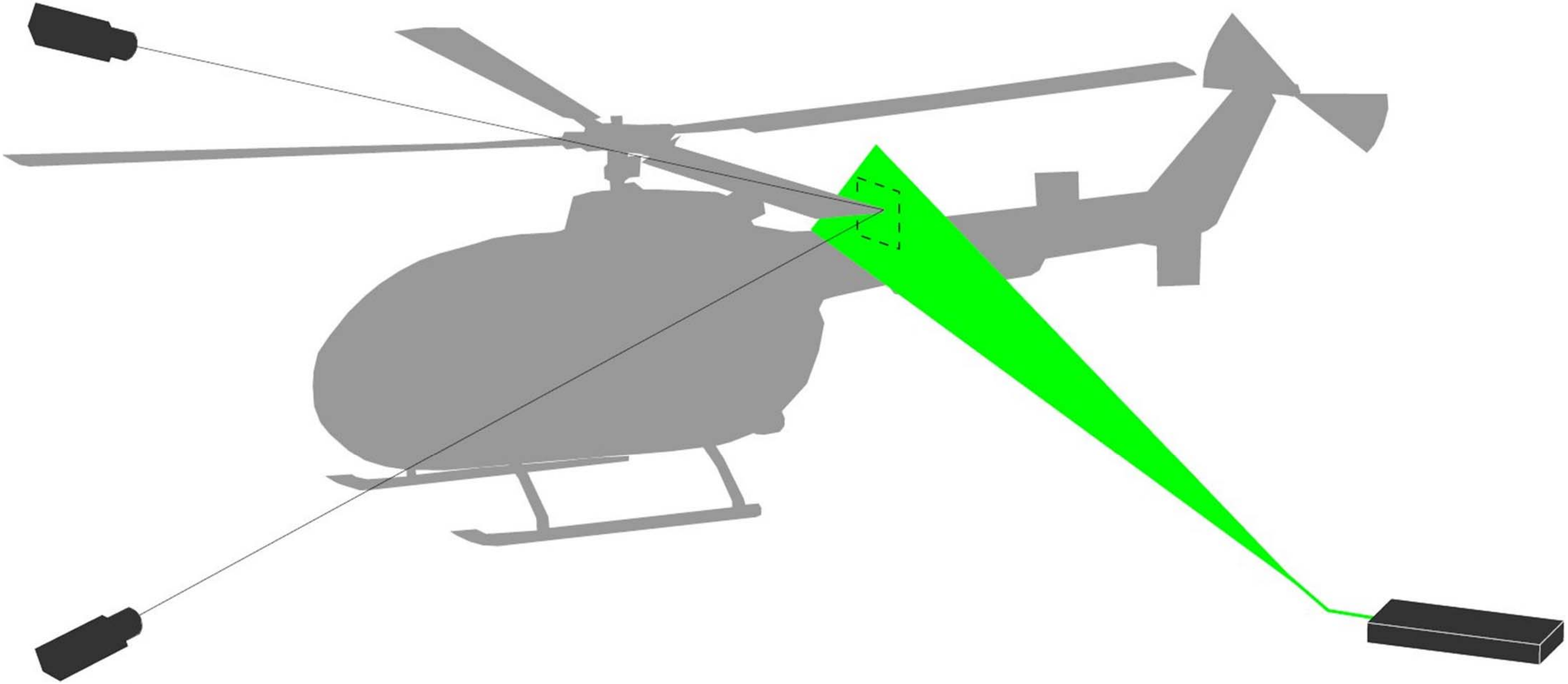

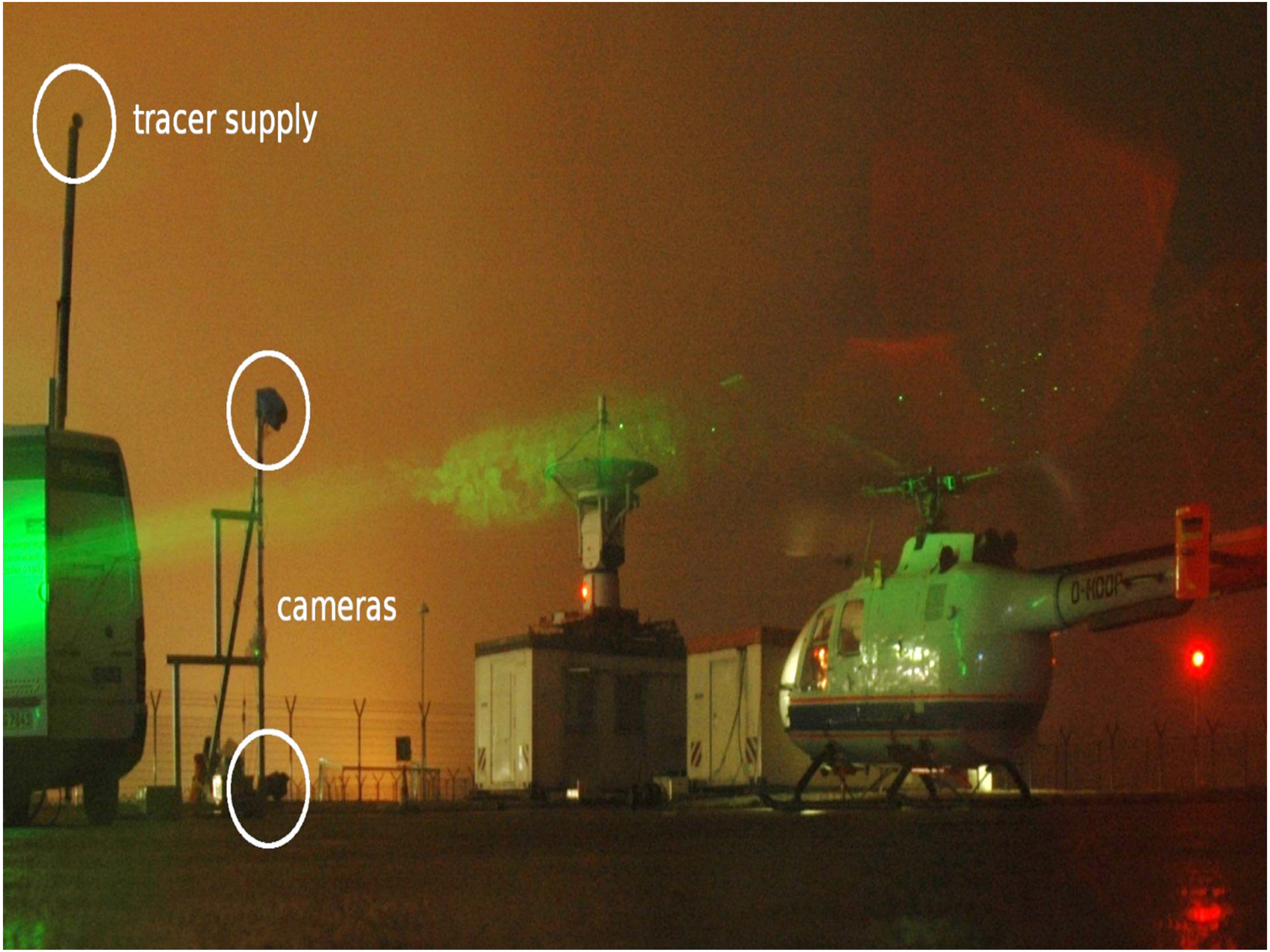
tracer supply
cameras
D-HOOP

The data quality has been significantly increased and allows for quantification of vortex core radius and swirl velocity at full scale in hover flight (IGE)

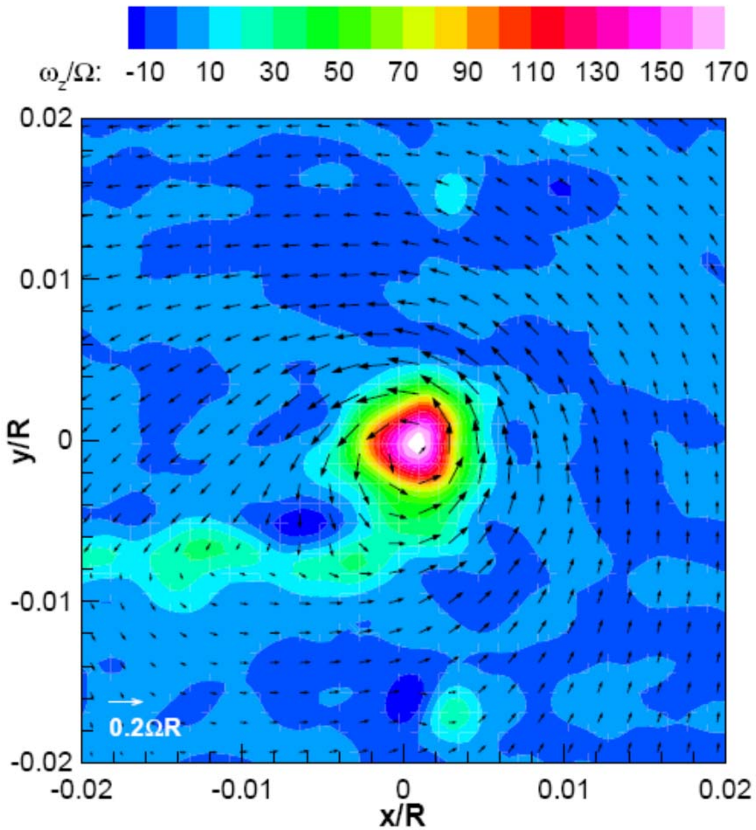

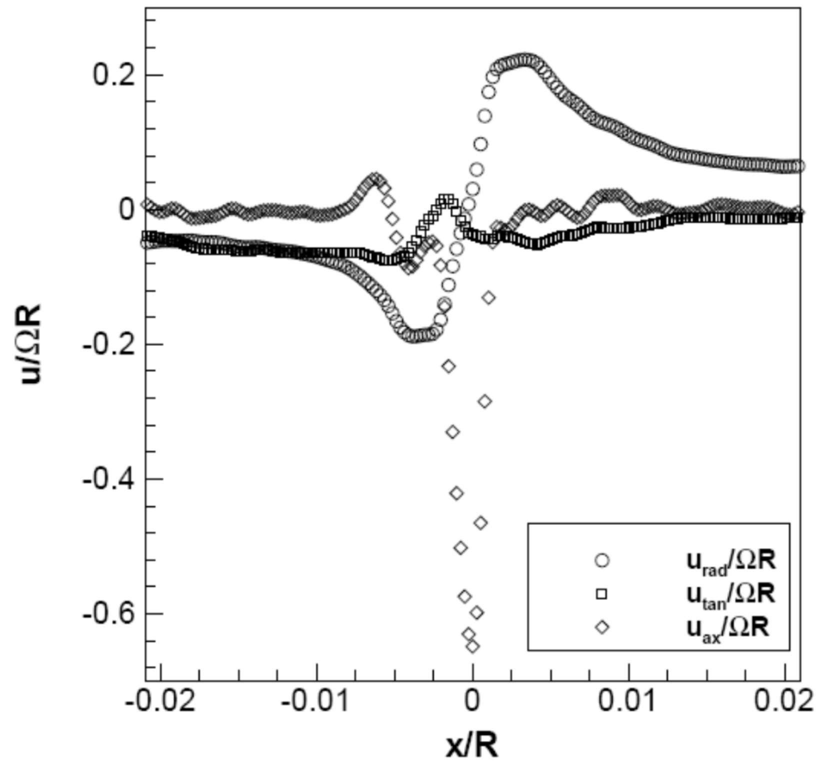

Background oriented schlieren method BOS

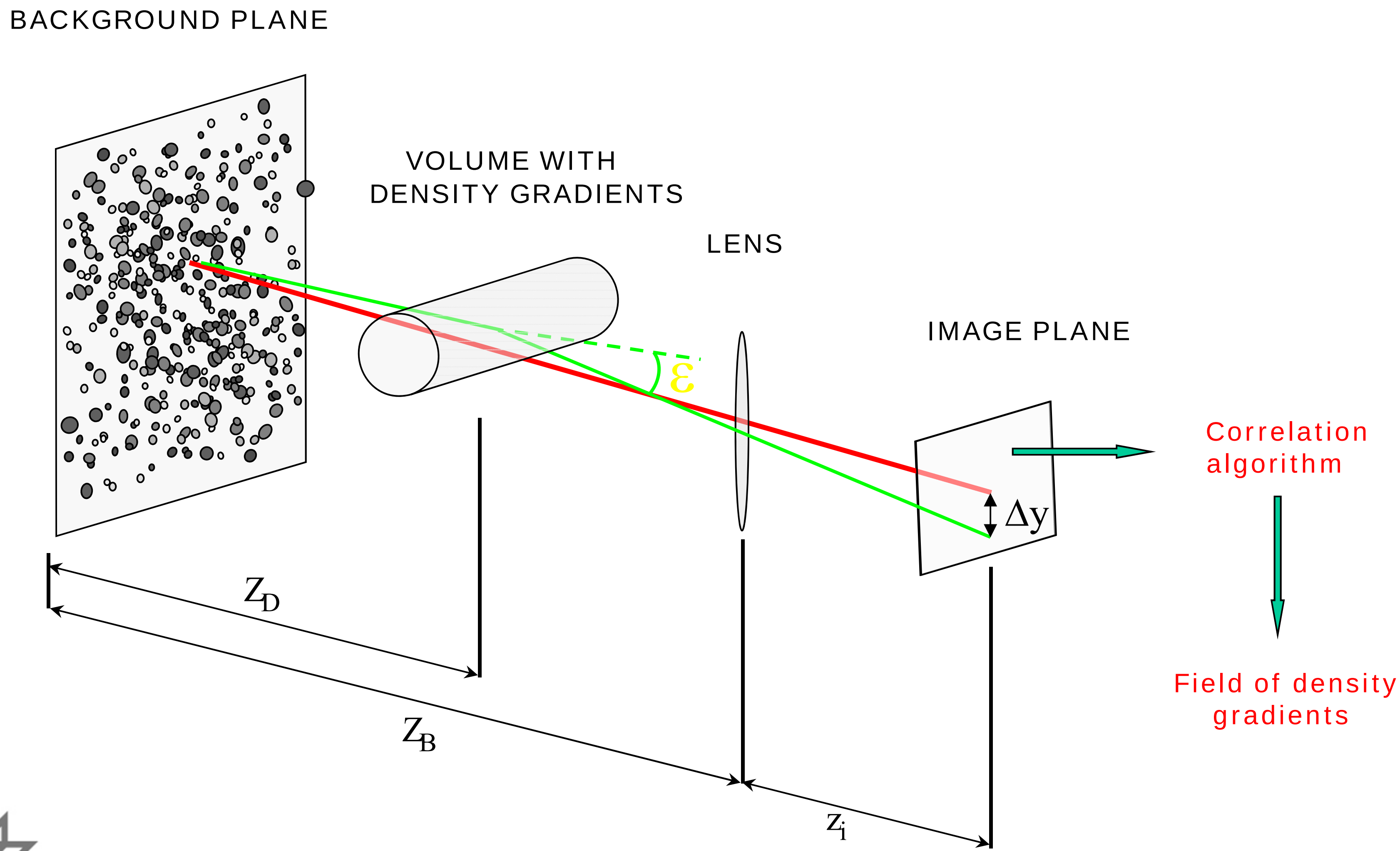

First application of BOS in 2000: Visualization of blade tip vortices in flight

BK117 (Eurocopter)

2 cameras with 1280 x 1024 Pixel (180 mm und 100 mm lenses)

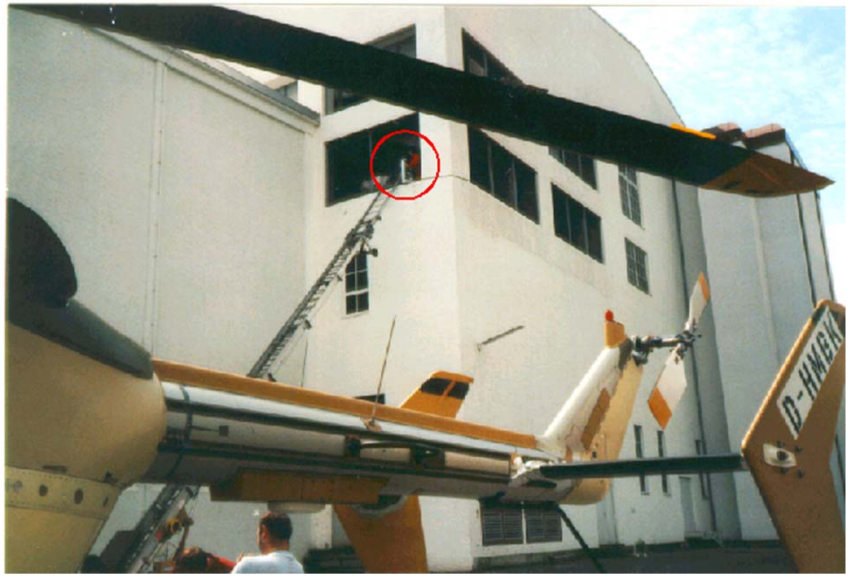

Camera position

Random dot patterns

Recording of the dot pattern during flight

Integration along the line of sight

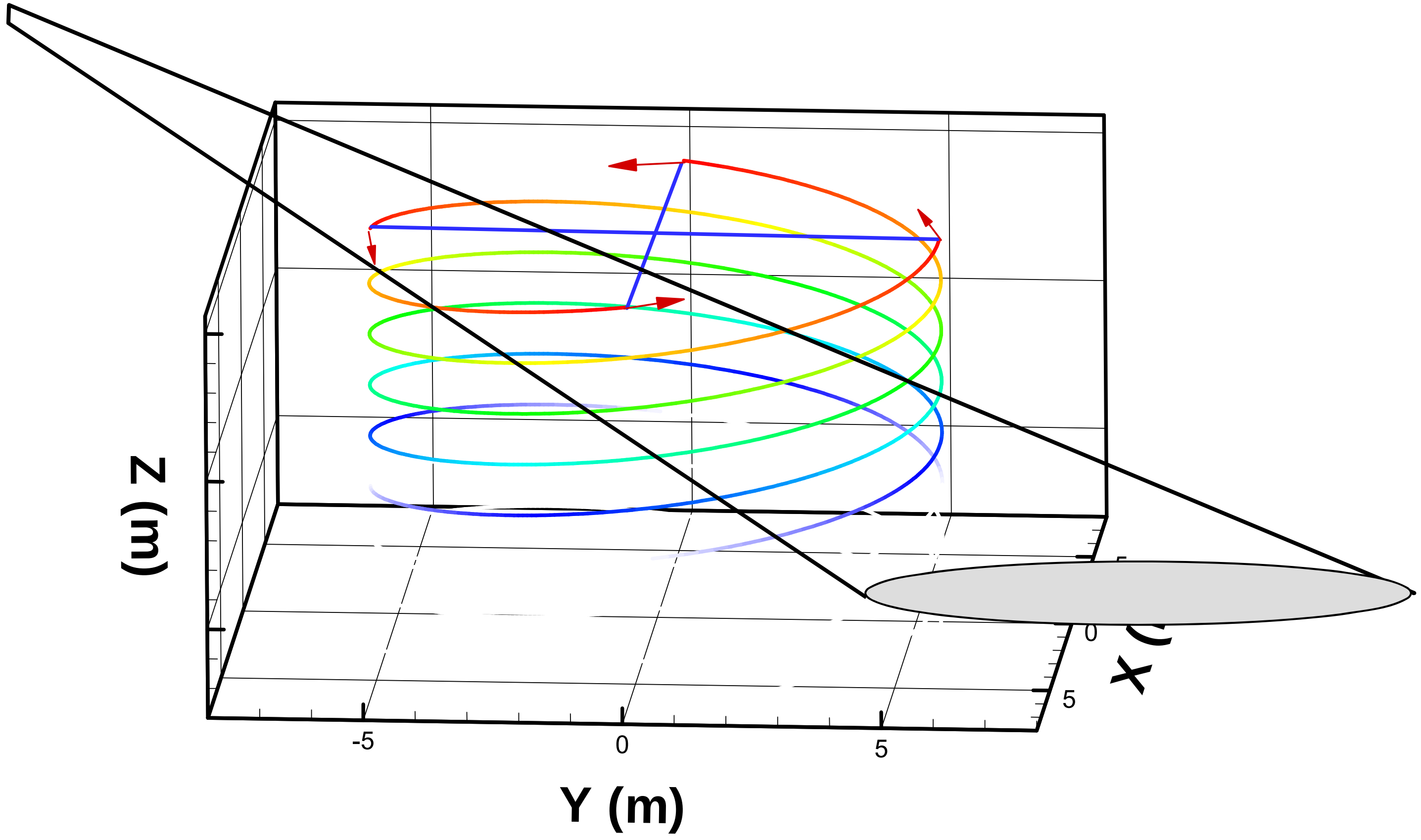

reference

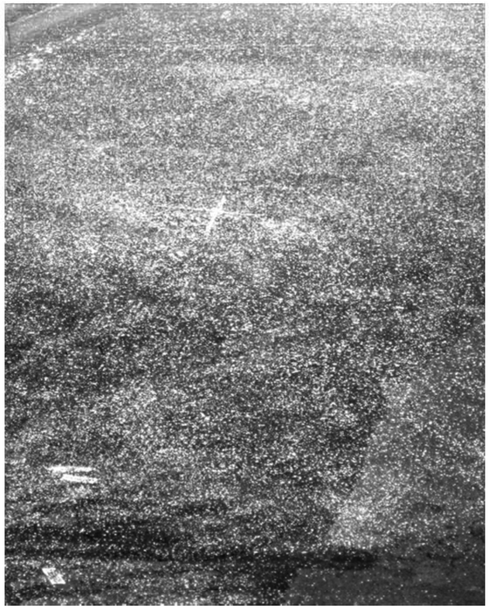

hover

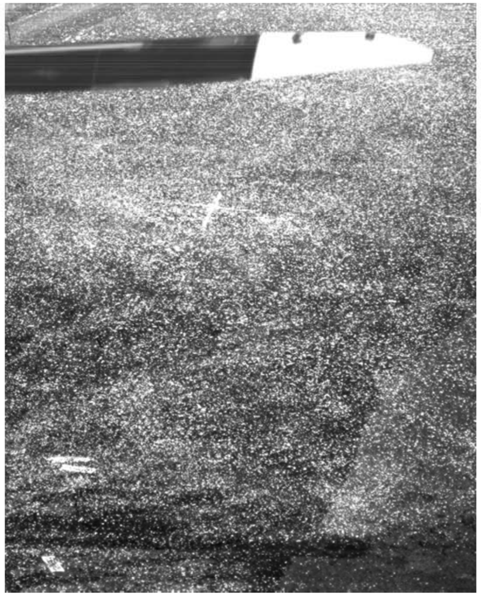

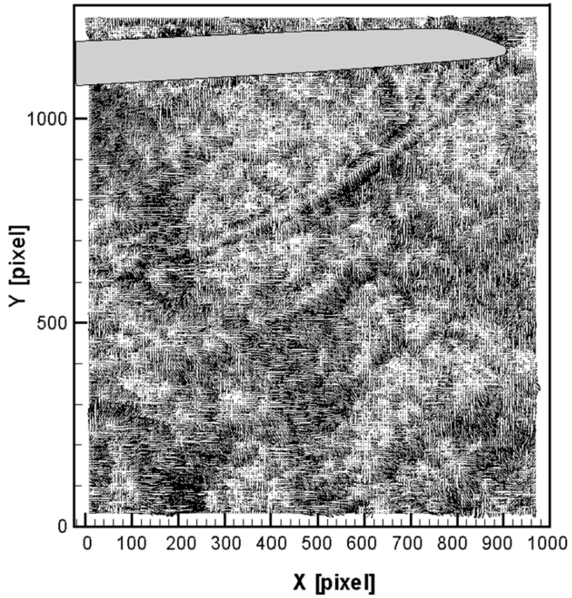

Results of the crosscorrelation
(100mm lens)

Results of the crosscorrelation
(180mm lens)

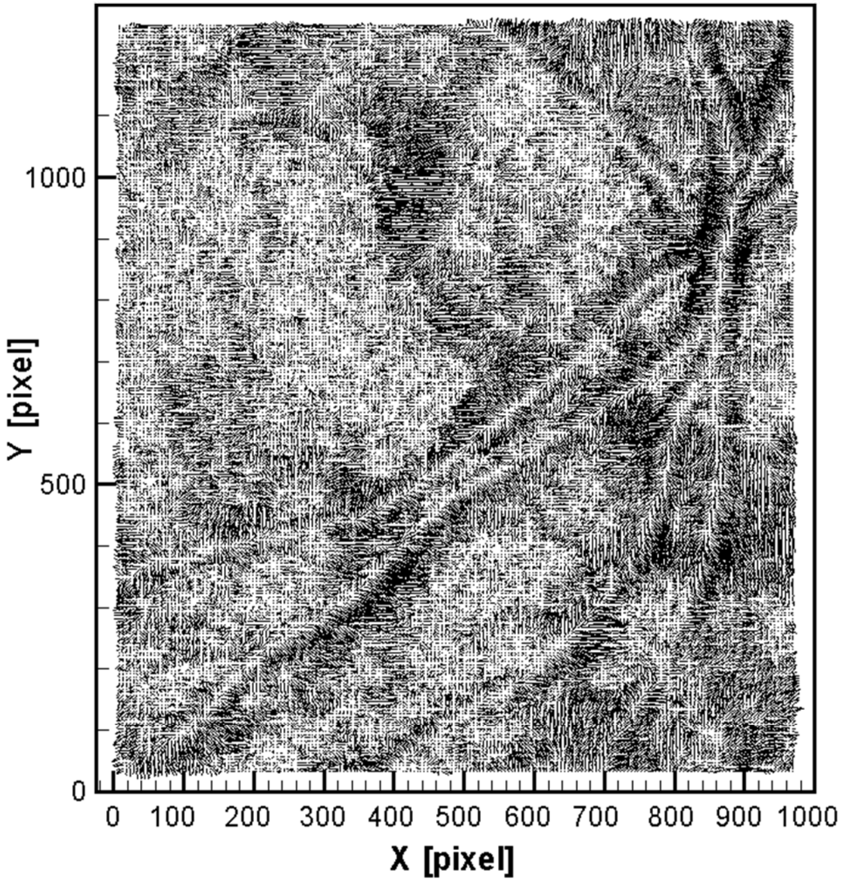

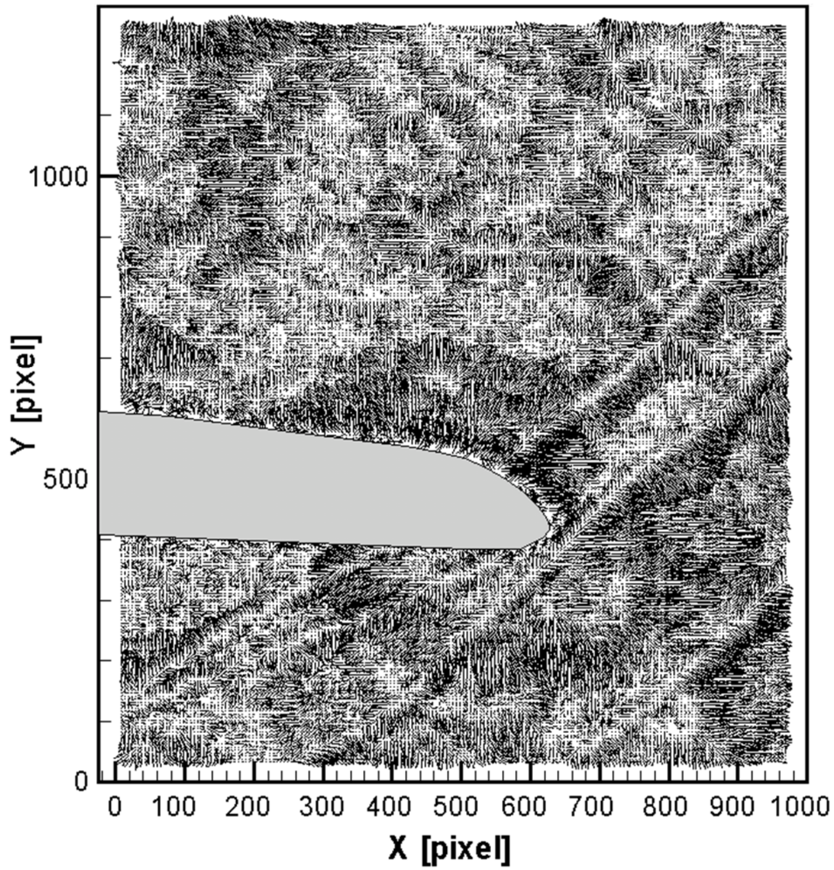

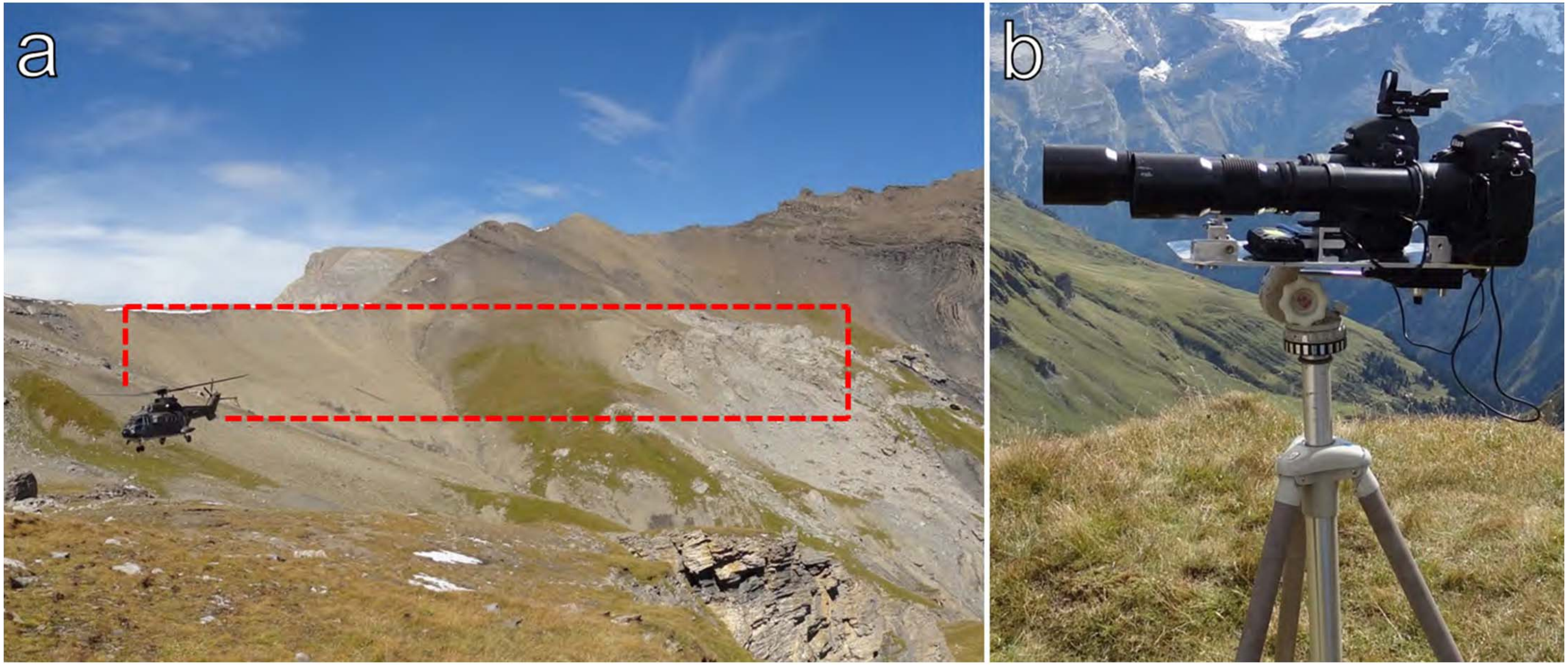

(a) View of the flight test region with the Cougar helicopter during take off. The area in red indicates the backgrounds used. (b) The paraxial reference-free BOS setup.

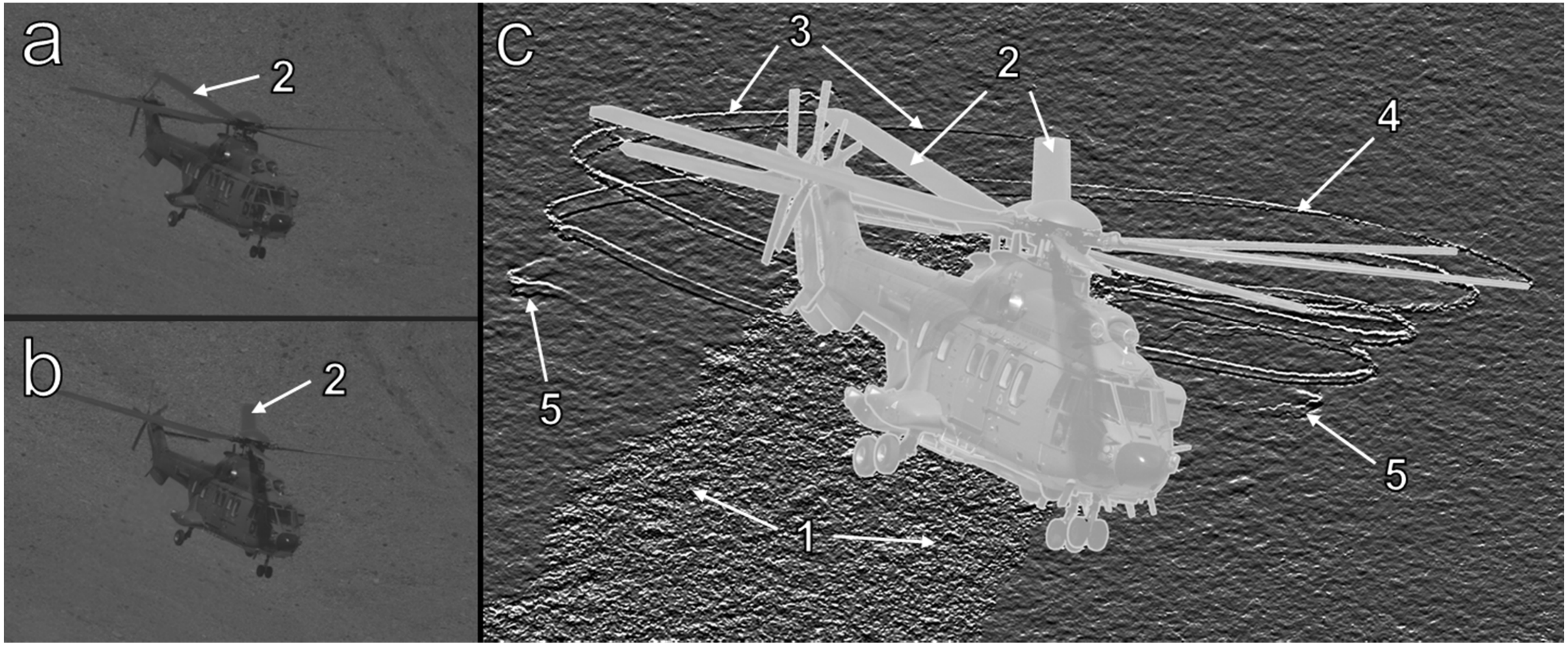

(a,b) Measurement images of the two paraxial cameras with a time delay of 16 ms.
(c) Evaluated image depicting the vertical displacement gradient field with the superimposed pictures of the helicopter.

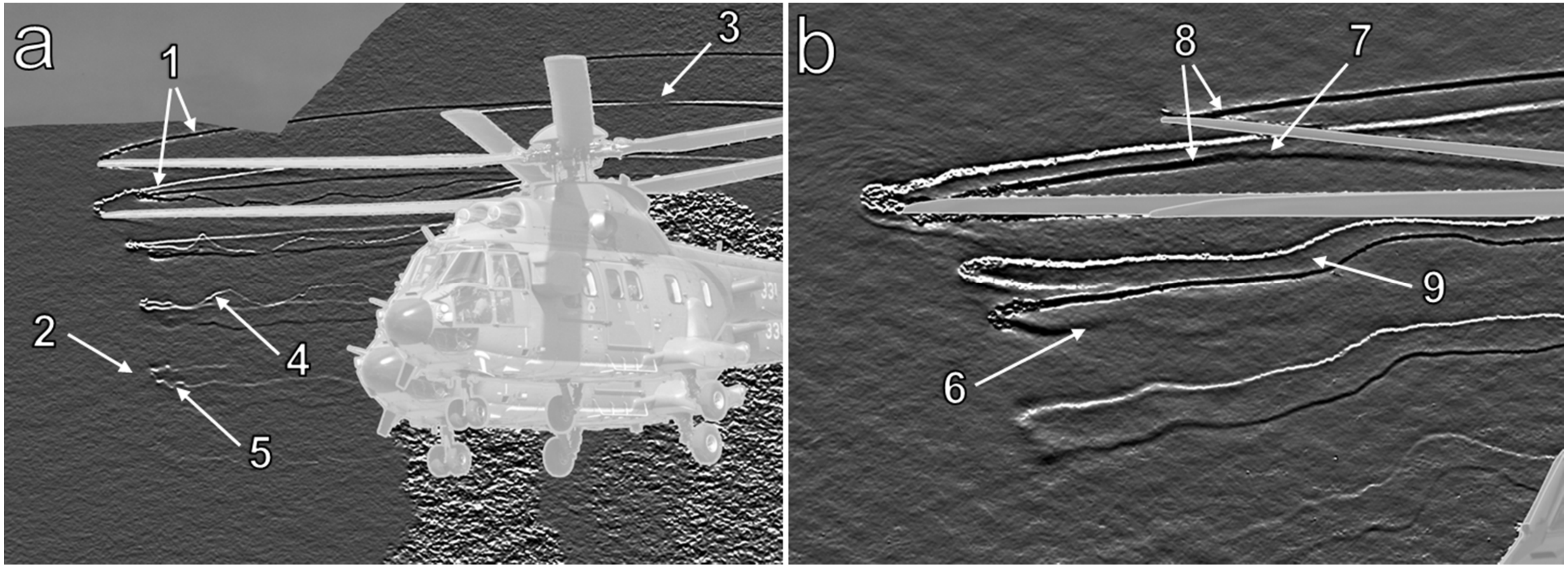

Comparison of the rotor wake of the hovering helicopter for (a) the monoscopic BOS setup and (b) the paraxial BOS setup.

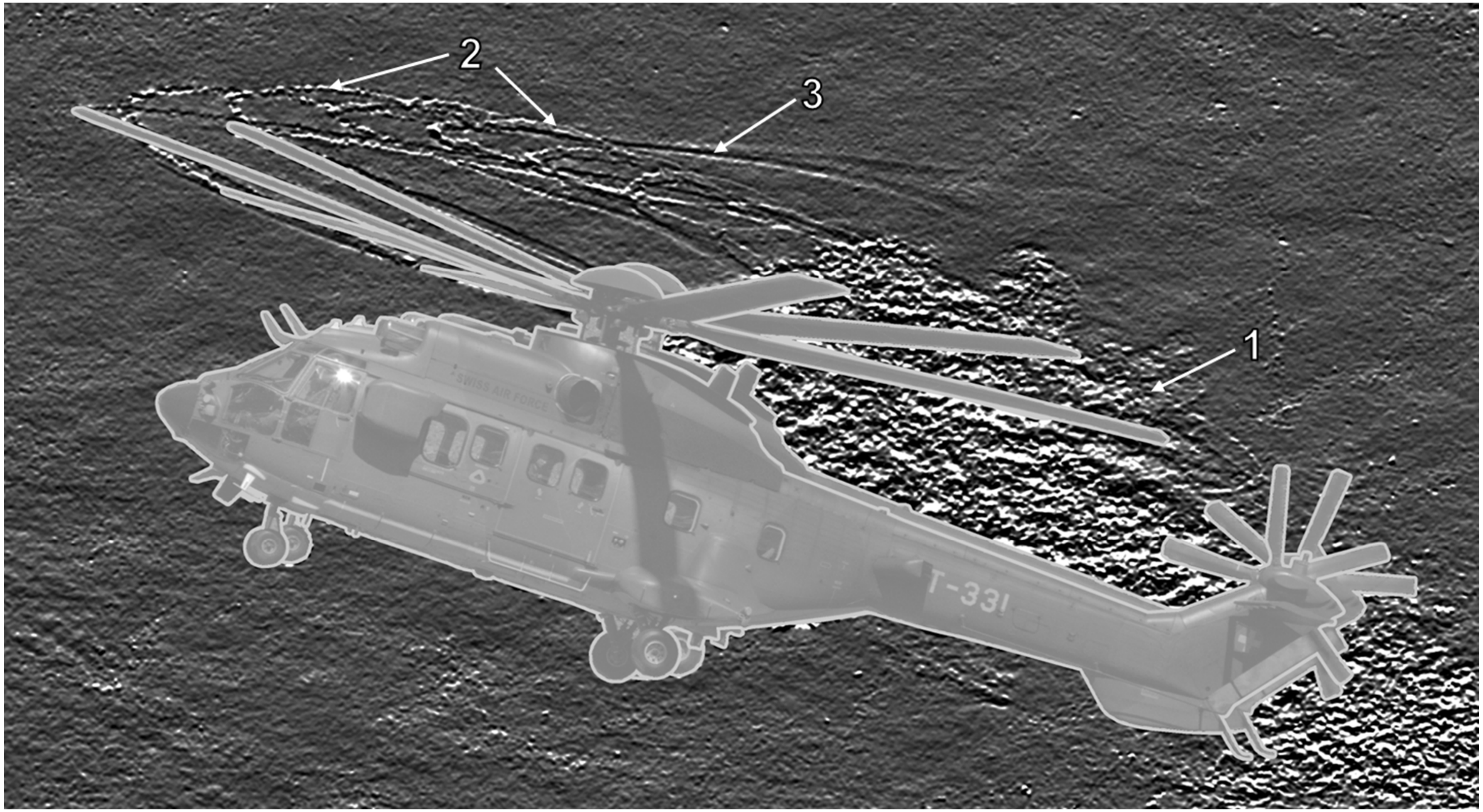

Evaluated image of the helicopter during a flare maneuver. (1) exhaust plumes, (2) multiple vortex filaments convecting downstream above the rotor plane, (3) vortices shed from the lateral edges of the rotor tip path plane.

test campaign with two helicopters and a 4-camera airborne BOS system

Tomographic measurements on DLR’s BO105 helicopter in hover flight conditions have been performed in order to derive the blade tip vortices density distributions.

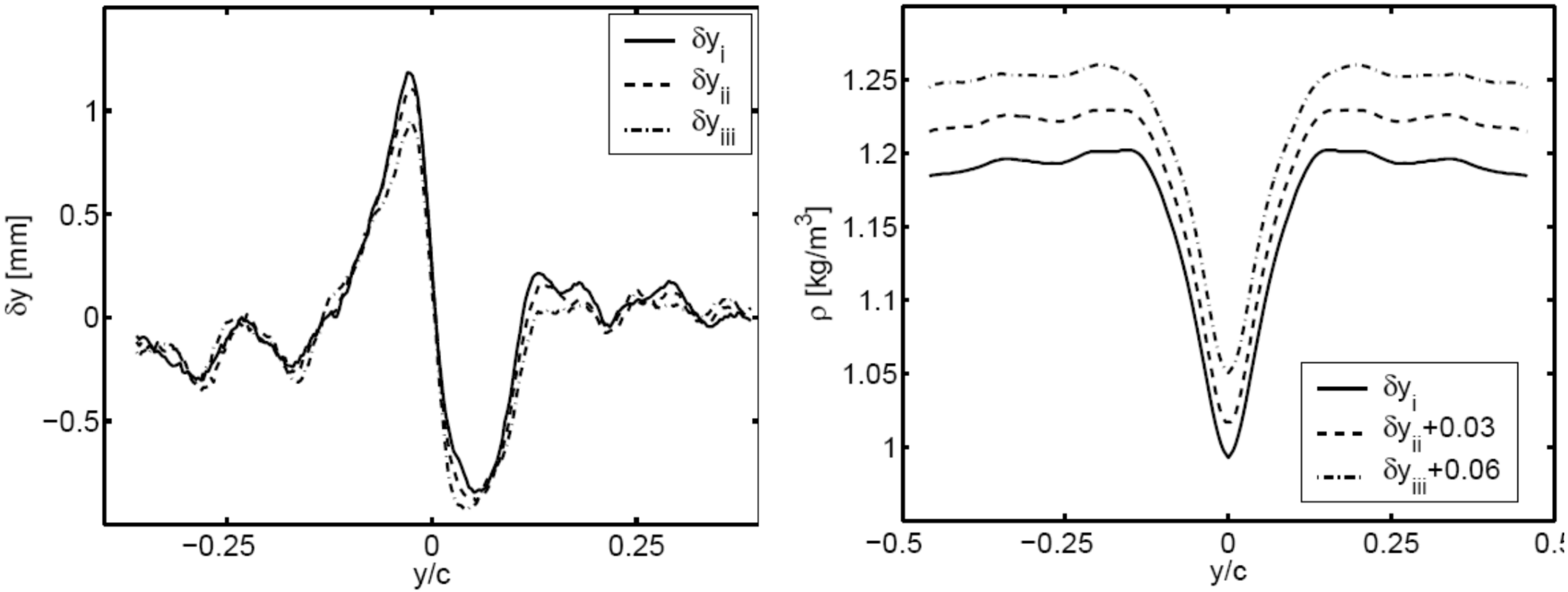

Figure BOS: Density gradient (left diagram) and the resulting tomographically evaluated density distribution (right digramm).

Computer Tomography

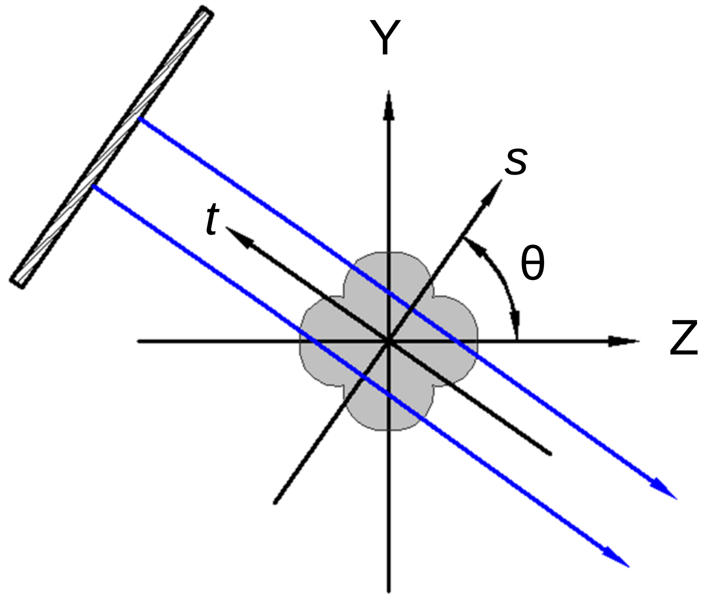

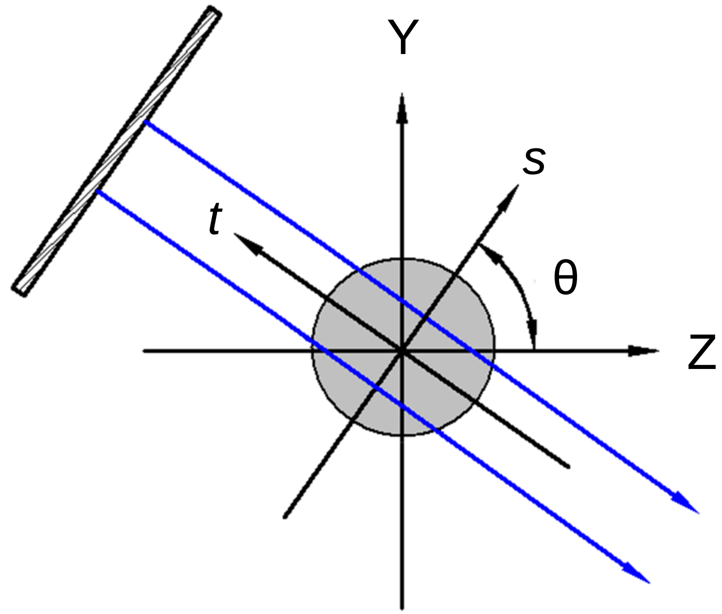

Quality of tomographic reconstruction in general:

- Number of recording projections.
- Angular range of 180˚.
- Density data per square unit.

Our assumptions:

- Axisymmetric flow.
- One recording projection.
- Same information repeated in the angular range of 180˚.

Liu, T.C., Merzkirch, W., and Oberste-Lehn, K. 1989

Airborne camera BOS recording

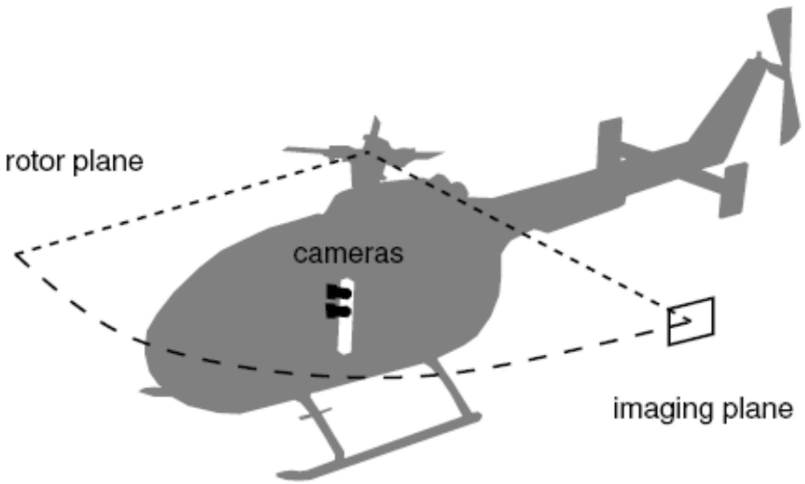

Tomographic BOS evaluation =>

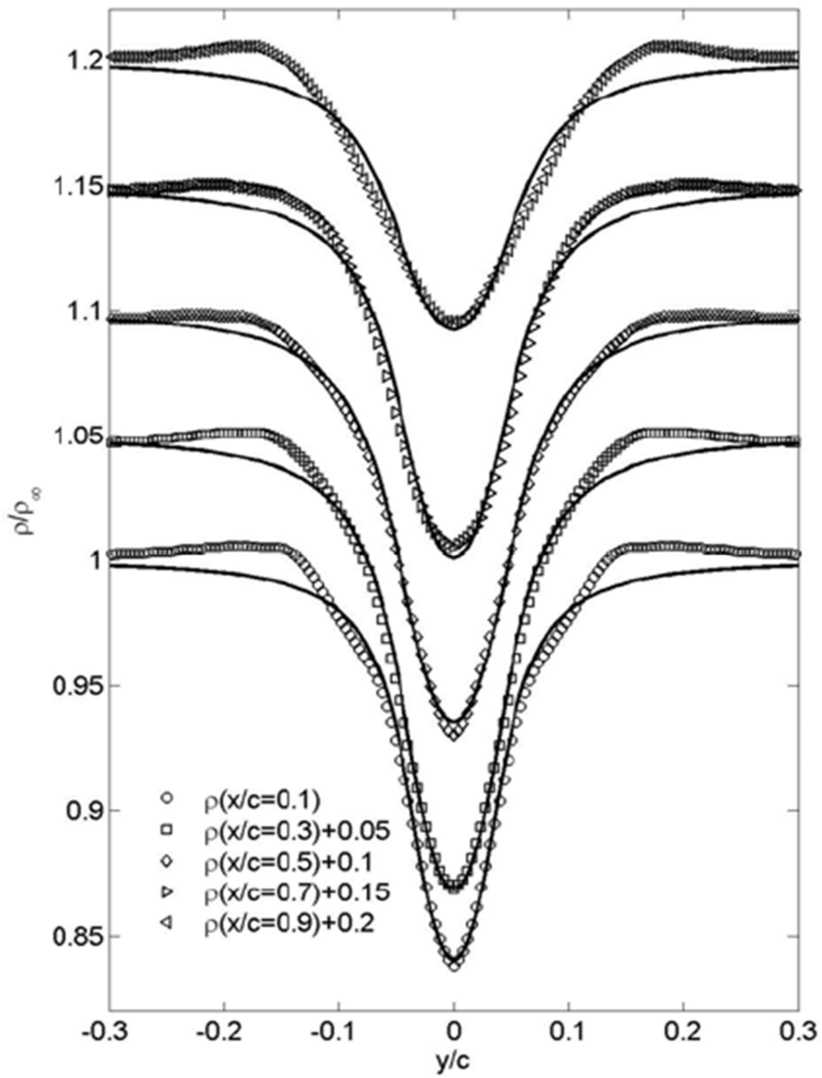

Flight Test Setup

- Flight tests with a BO105 in a quarry in the Harz Mountains
- …cquisition with 10 ca…

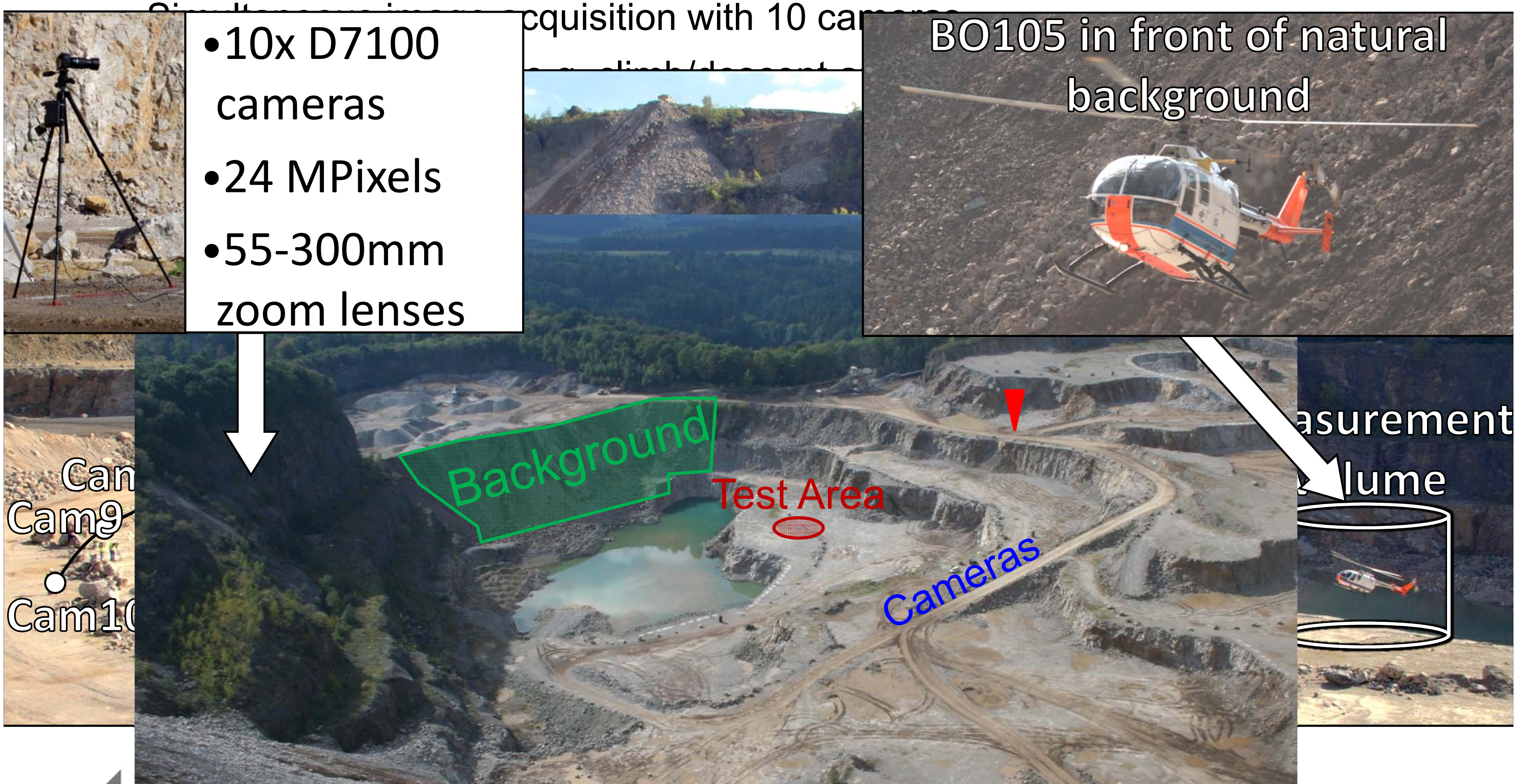

Flight Test Setup

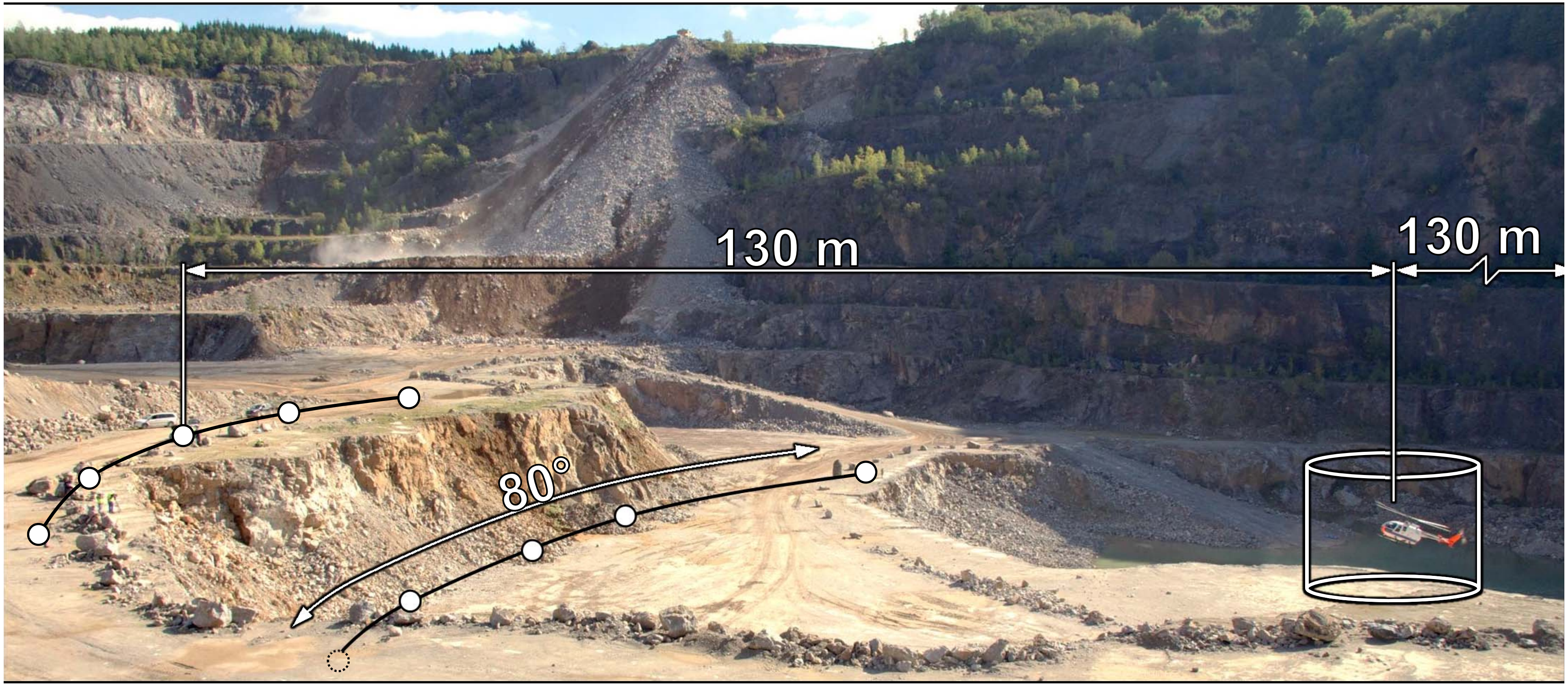

Vortex Visualization – Climb

Image Acquisition and Processing

- Acquisition of undisturbed reference and measurement image
- Mapping of images to compensate for eventual misalignments

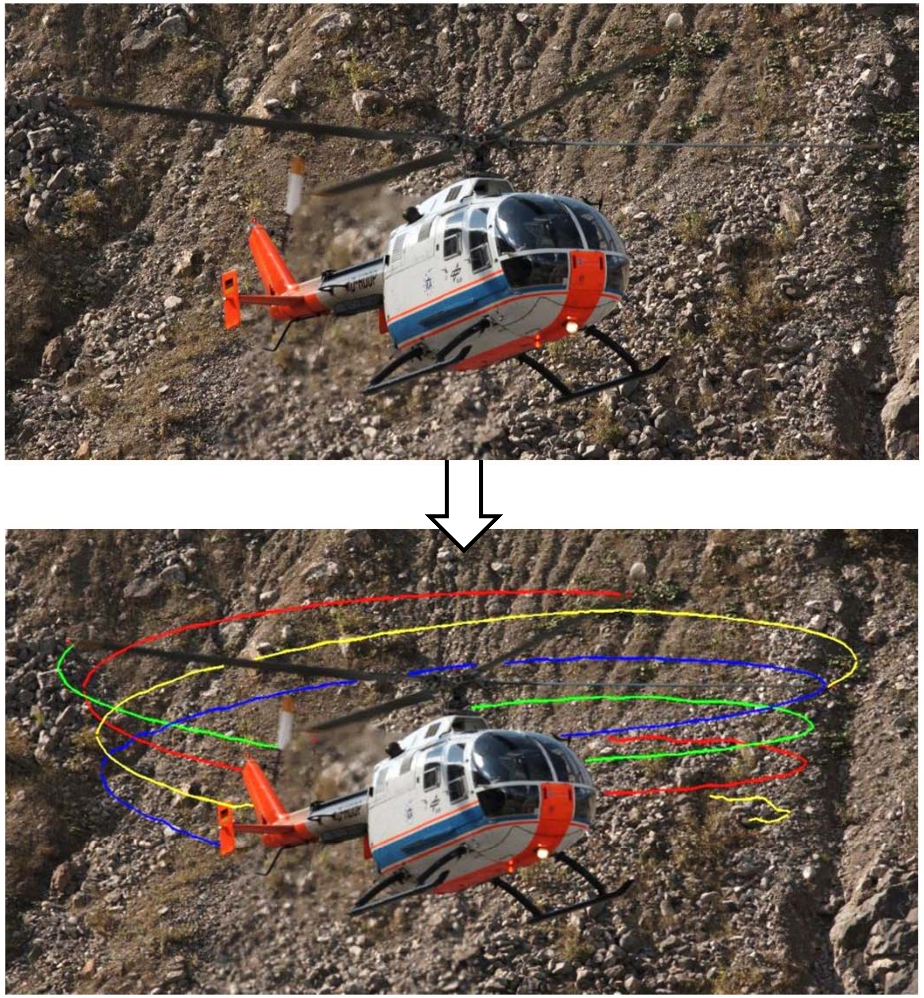

- Stepwise cross-correlation between images
- Semi-automatic 2D vortex extraction and spline fitting

Vortex Visualization – Climb

- Vortex visualization for ascending flig
- Maximum visible vortex age: ~ 360°

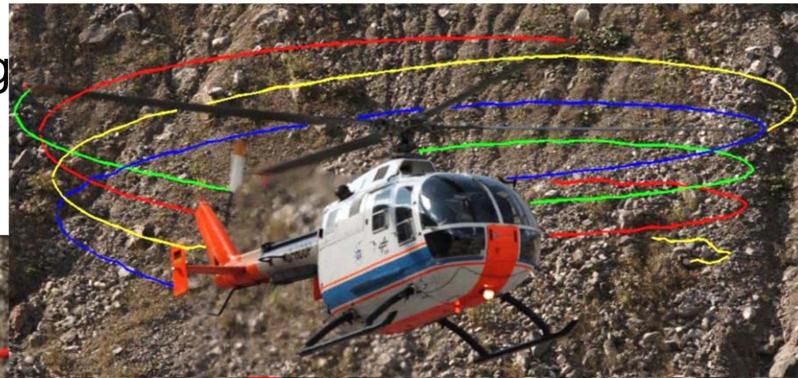

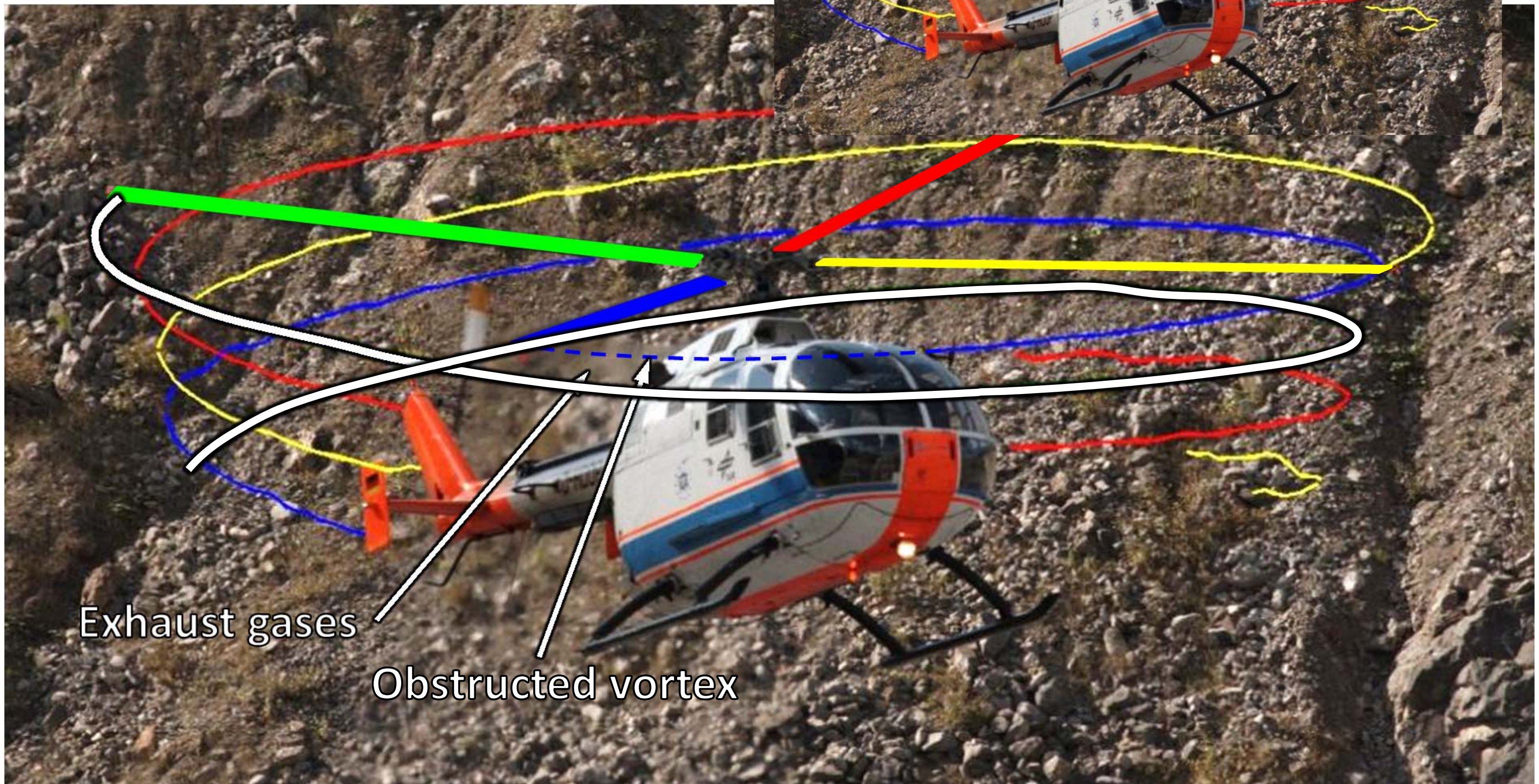

Vortex Visualization – Climb

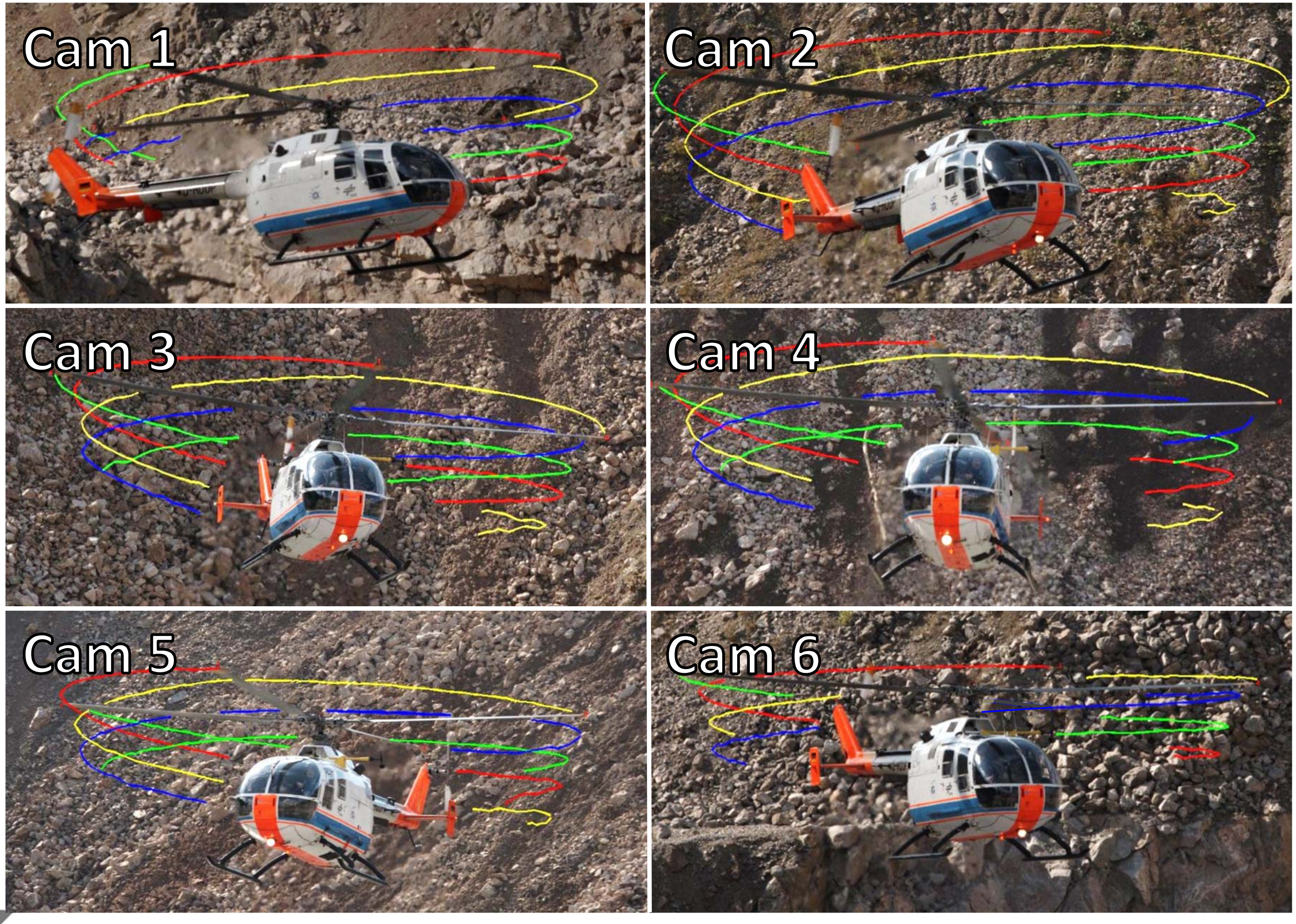

Results – 3D Vortex Reconstruction

- 3D
- Ba

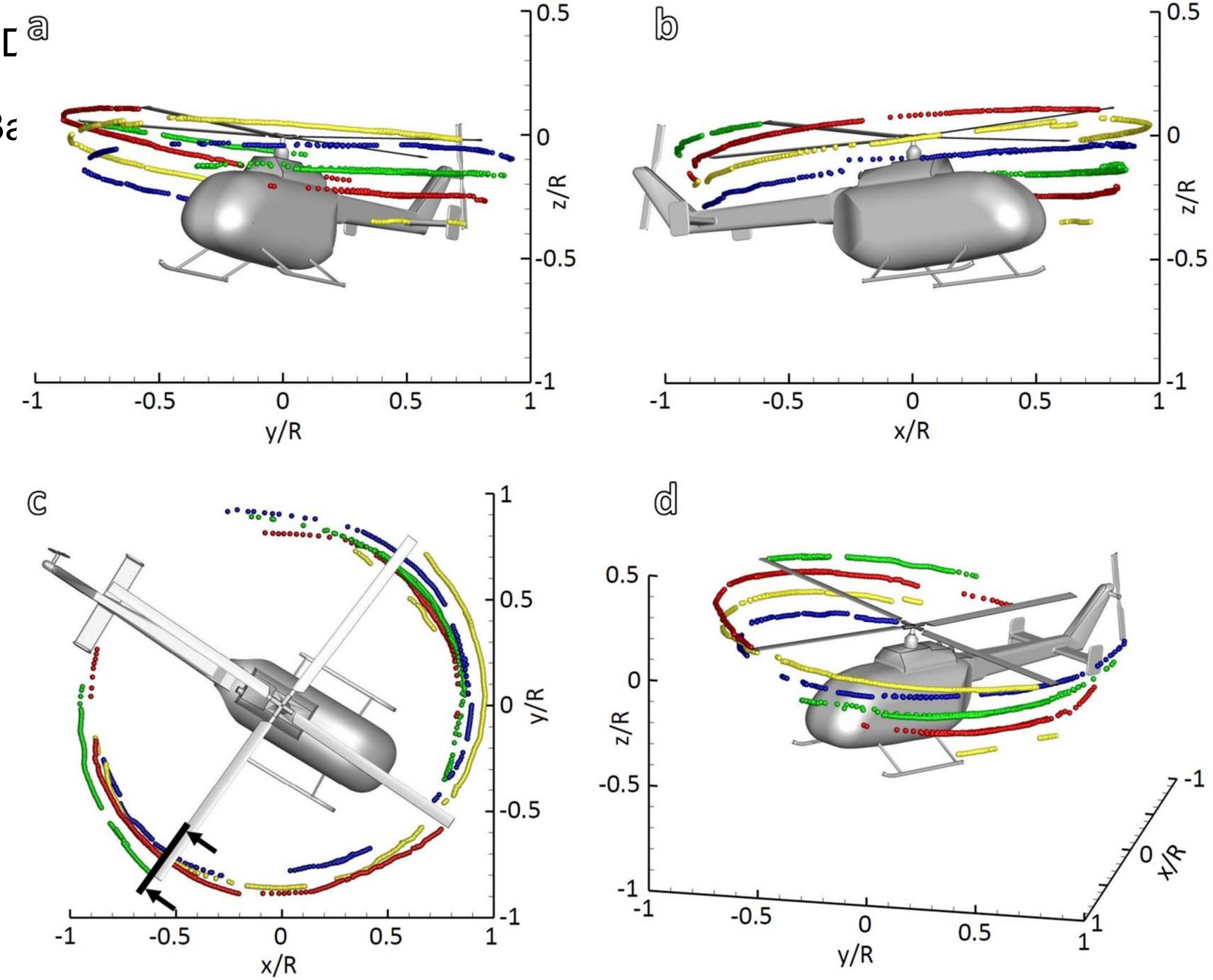

Results – 3D Vortex Reconstruction

- Radial cut section through vortex system
- Quantitative geometric information about positions of blades and vortices

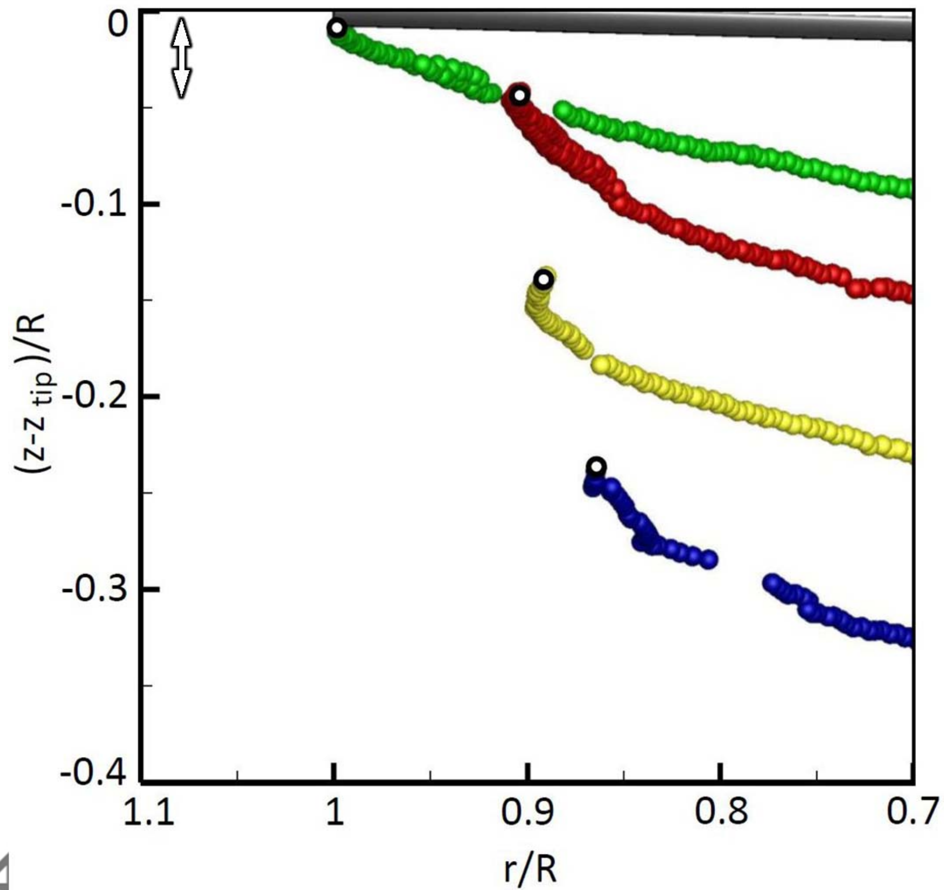

- Blade-vortex miss-distance: 0.8 c at r / R = 0.905 with an interaction angle of close to 90°

→Demonstration of capability of BOS method to determine important geometric factors for blade vortex interaction effects

Results – 3D Vortex Reconstruction

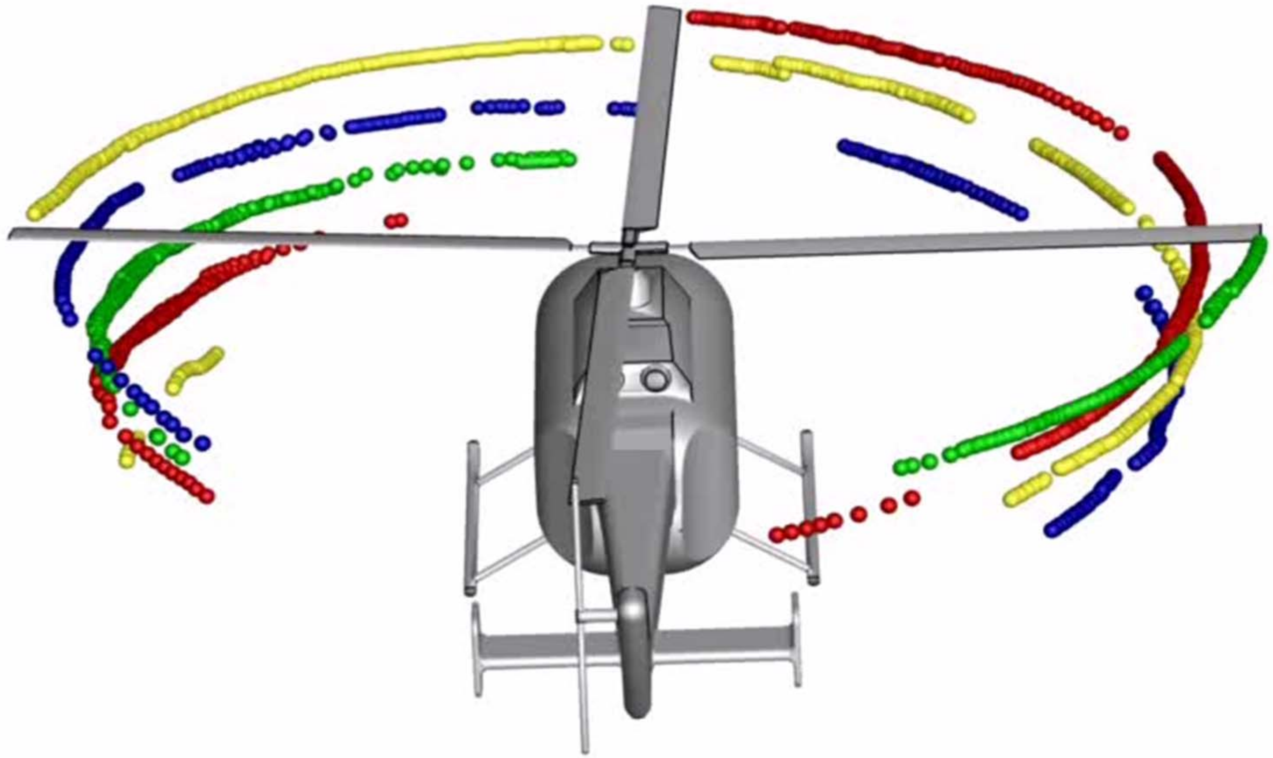

Conclusion

- Two optical techniques have been developed and applied in large scale wind tunnel experiments and flight tests for CFD code validation.

- Particle Image Velocimetry is mainly suited for it's application in wind tunnels, because of the need of tracer particles. It delivers accurate velocity data with high spatial and temporal resolution.

- Background Oriented Schlieren techniques can be used in flight tests in order to obtain vortex lcations and density data from helicopters in maneuvering flight.